



**MARCIN STEFAN
CWIKLINSKI**

**IMPEDANCE CONTROL OF A HYDRAULIC
SERVOMECHANISM**



**MARCIN STEFAN
CWIKLINSKI**

**IMPEDANCE CONTROL OF A HYDRAULIC
SERVOMECHANISM**

dissertação apresentada à Universidade de Aveiro, ao abrigo do programa Erasmus, realizada sob a orientação científica do Prof. Dr. Jorge Augusto Fernandes Ferreira, Professor Auxiliar do Departamento de Engenharia Mecânica da Universidade de Aveiro.

o júri

Presidente

Doutor Fernando José Neto da Silva
Professor Auxiliar da Universidade de Aveiro

Arguente

Doutor Raul Morais dos Santos
Professor Auxiliar da Universidade de Trás-os-Montes e Alto Douro

Orientador

Prof. Dr. Jorge Augusto Fernandes Ferreira
Professor Auxiliar da Universidade de Aveiro

agradecimientos

I would like to express my gratitude for Dr Jorge Augusto Fernandes Ferreira for the help and support during the whole process of writing my master thesis. His directions and encouragements were priceless and always helpful. I would also like to thank Dr Rafal Zawislak, from Technical University of Lodz, who agreed to read and evaluate my work.

palavras-chave

Controlo de impedância, controlo de posição, controlo de força, servomecanismo hidráulico, controlador PID, controlo baseado em lógica difusa.

resumo

No presente trabalho é proposto e implementado um controlador de impedância baseado na posição para o controlo de um cilindro, instalado numa prensa hidráulica, comandado por uma servoválvula actuada por solenóide. Foram inicialmente desenvolvidos controladores de posição, controlador PID e controlador baseado em lógica difusa, com os requisitos de precisão adequados à implementação do controlador de impedância baseado na posição. O filtro de impedância foi colocado na malha de realimentação de força para modificar a trajectória do actuador hidráulico de acordo com o comportamento especificado. Simultaneamente com as experiências na prensa hidráulica, o controlo de impedância foi experimentado em ambiente totalmente simulado recorrendo a um modelo não linear de todo o sistema hidráulico (cilindro + servoválvula). Foram realizadas várias experiências em espaço livre e em contacto com o ambiente. Foram conseguidos resultados satisfatórios em ambas as situações bem como na transição de não-contacto para contacto com o ambiente.

keywords

Impedance control, position control, force control, hydraulic servomechanism, PID controller, Fuzzy Logic Controller.

abstract

A position-based impedance controller is proposed and demonstrated on an existing hydraulic press with a two-way vertically mounted hydraulic cylinder driven by a servo-solenoid valve. A proportional-integral-derivative (PID) controller and a Fuzzy Logic Controller (FLC) are primarily developed to meet the accurate positioning requirements of the impedance control formulation. The impedance filter was placed in force-feedback loop to modify a desired trajectory of the hydraulic actuator according to a specified behavior. Simultaneously with the experiment conducted on the real hydraulic press, impedance control was performed in computer simulation with the use of a non-linear model of the whole hydraulic system (cylinder + servo solenoid valve). Experiments were carried out in free space and with environmental contact. Satisfactory results were achieved in both situations, as well as in non-contact/contact transition.

Table of Contents

| | |
|---|-----|
| Notation..... | iii |
| Subscripts..... | v |
| Abbreviations..... | vi |
| List of Figures..... | vii |
| Thesis overview..... | ix |
| Chapter 1 Introduction..... | 1 |
| 1.1. History..... | 1 |
| 1.1.1. Hydraulic systems – characteristics..... | 1 |
| 1.1.2. Control of Hydraulic Systems..... | 4 |
| 1.2. Impedance Control..... | 8 |
| 1.3. Organization..... | 10 |
| Chapter 2 Experimental Test Platform..... | 11 |
| 2.1. Hardware..... | 11 |
| 2.2. Instrumentation..... | 13 |
| 2.3. Data Acquisition and Control..... | 14 |
| Chapter 3 Modeling of the System..... | 16 |
| 3.1 Nonlinear Model..... | 16 |
| 3.1.1. Valve Model..... | 17 |
| 3.1.1.1. Dynamic Model – Spool Motion..... | 17 |
| 3.1.1.2. Static Model - Volumetric Flowrate Model..... | 19 |
| 3.1.2. Hydraulic Cylinder Model..... | 21 |
| 3.1.2.1. Piston dynamics..... | 21 |
| 3.1.2.2. Effective bulk modulus..... | 23 |
| 3.1.2.3. Friction model..... | 23 |
| 3.2 Parameterization..... | 25 |
| Chapter 4 Implementation of the Impedance Controller..... | 28 |
| 4.1. Real System..... | 29 |
| 4.2. Simulation..... | 32 |
| 4.3. Position Control..... | 33 |
| 4.3.1. PID Controller..... | 33 |
| 4.3.2. Fuzzy Logic Controller..... | 34 |

| | |
|--|----|
| 4.3.2.1. Fuzzy Membership Function | 36 |
| 4.3.2.2. Fuzzification | 36 |
| 4.3.2.3. Reasoning – fuzzy rule base | 37 |
| 4.3.2.4. Defuzzification..... | 38 |
| 4.3.2.5. Fuzzy Logic Control Surface | 39 |
| 4.3.2.6. Fuzzy Logic Controller in Simulink® | 39 |
| Chapter 5 Experimental results..... | 41 |
| 5.1. Position Control | 42 |
| 5.2. Impedance Control..... | 45 |
| 5.2.1. Position trajectory - PID controller..... | 46 |
| 5.2.2. Position trajectory – Fuzzy Logic Controller..... | 49 |
| 5.2.3. Position trajectory – PID v FLC | 52 |
| 5.2.4. Hydraulic pressure in chamber A and B | 55 |
| 5.3. Results Evaluation | 56 |
| Chapter 6 Conclusion | 58 |
| References..... | 61 |

Notation

| | |
|----------------|---|
| A | area or section |
| a_p | piston acceleration |
| B | damping factor for dashpot |
| F, f | force |
| f_c | Coulomb friction force |
| f_s | Stribeck effect or friction force |
| f_v | viscous friction force |
| k_v | viscous friction coefficient |
| \bar{K}_{p0} | relative pressure gain at $\bar{x}_s = 0$ |
| \bar{K}_{q0} | flow gain at $\bar{x}_s = 0$ |
| K | gain |
| K_s | spring rate |
| L_v, L_a | valve spool velocity and acceleration limits |
| M | mass |
| P | relative pressure |
| ΔP | relative pressure difference |
| P_L | relative pressure under load |
| \bar{P}_L | relative pressure difference under load |
| P_n | nominal pressure difference |
| Q, q | volumetric flow rates |
| Q_L | volumetric flow rate under load |
| Q_n | nominal volumetric flow rate |
| t | time |
| T | temperature |
| u | control signal |
| \bar{u} | normalized control signal, $\bar{u} \in [-1,1]$ |
| V | volume |
| V_L | volume of transmission lines |
| v_p | piston velocity |
| x_p | piston position |

| | |
|-------------|---|
| \bar{x}_p | normalized piston position, $\bar{x}_p \in [-1,1]$ |
| \bar{x}_s | normalized valve spool position, $\bar{x}_s \in [-1,1]$ |
| ζ | damping factor |
| β_e | effective bulk modulus |
| ω | angular frequency |
| ω_c | angular cutoff frequency |
| ω_n | natural angular frequency |
| Δt | time delay |

Subscripts

| | |
|------------|-------------------------------|
| <i>0</i> | value at zero |
| <i>i</i> | initial value |
| <i>in</i> | input or entry value |
| <i>ij</i> | from i to j |
| <i>f</i> | final value |
| <i>k</i> | discrete value |
| <i>lam</i> | laminar flow region |
| <i>lk</i> | leaks |
| <i>max</i> | maximum value |
| <i>min</i> | minimum value |
| <i>out</i> | output or exit value |
| <i>ref</i> | reference value |
| <i>s</i> | source (for flow or pressure) |
| <i>ss</i> | steady state value |
| <i>T</i> | turbulent flow region |
| <i>t</i> | tank (for flow and pressures) |
| <i>v</i> | valve |

Abbreviations

| | |
|------|--|
| COG | Centro of Gravity |
| FLC | Fuzzy Logic Control |
| ISE | Integrated Squared Error |
| MAST | Multi-Axial Subassemblage Testing |
| LQR | Linear Quadratic Regulator Control |
| MRAC | Model Reference Adaptive Control |
| MRC | Model Reference Control |
| MPC | Model-based Predictive Control |
| P | Proportional Control |
| PI | Proportional Integral Control |
| PID | Proportional Integral Derivative Control |
| RTW | Real-Time Workshop |

List of Figures

| | |
|---|----|
| Figure 1: Comparison of electromechanical and hydraulic system response times | 2 |
| Figure 2: Picture of Hydraulic Press | 11 |
| Figure 3: (left) Upper cylinder, valve, load cell and position sensor..... | 12 |
| Figure 4: (right) Lower cylinder and valve..... | 12 |
| Figure 5: Hydraulic circuit of prototype hydraulic press [Ferreira02] | 13 |
| Figure 6: DS1102 DSP Comp. Card setup for data acquisition and control..... | 14 |
| Figure 7: <i>ControlDesk</i> graphical user interface for impedance control..... | 15 |
| Figure 8: Division of the valve model (dynamic model and static model)..... | 17 |
| Figure 9: 2 nd order model with delay to compensate the phase [Quintas99]..... | 18 |
| Figure 10: Bode plot of response for $\pm 5\%$ and 100% of valve spool range. | 18 |
| Figure 11: Block diagram of control valve dynamic model [Ferreira03]..... | 19 |
| Figure 12: Diagram of controlled valve..... | 19 |
| Figure 13: Diagram of control valve and hydraulic cylinder..... | 21 |
| Figure 14: Diagram of the friction between seal and cylinder wall..... | 24 |
| Figure 15: Simulink block diagram for simulation in open loop..... | 26 |
| Figure 16: Model and real system response to the applied step signal | 26 |
| Figure 17: Model and real system response to the applied sinusoid signal | 27 |
| Figure 18: Position-based impedance controller..... | 28 |
| Figure 19: Force-based impedance controller..... | 29 |
| Figure 20: Simulink [®] block diagram for RTW with impedance controller..... | 30 |
| Figure 21: <i>ControlDesk</i> interface..... | 31 |
| Figure 22: Simulink [®] block diagram with a model of hydr. system for simulation | 32 |
| Figure 23: The Simulink [®] block diagram of the feedback loop position control | 33 |
| Figure 24: The Simulink [®] block diagram of PID scheme for position control | 34 |
| Figure 25: Architecture of the Fuzzy Logic Controller [Cho04]..... | 36 |
| Figure 26: (right) Overall membership function plot for derivative of the error input | 36 |
| Figure 27: (left) Overall membership function plot for error input..... | 36 |
| Figure 28: (left) Example of fuzzification for error = -0.1 | 37 |
| Figure 29: (right) Example of fuzzification for derivative of the error = 0.2 | 37 |
| Figure 30: Fuzzy Logic Controller rule base | 38 |
| Figure 31: Centroid Defuzzification of the Result of Aggregation Process | 39 |

| | |
|---|----|
| Figure 32: Fuzzy Logic Control Surface | 39 |
| Figure 33: Simulink block diagram of the Fuzzy Logic Controller..... | 39 |
| Figure 34: Position control - step input signal | 42 |
| Figure 35: Position control - step input signal (zoom) | 42 |
| Figure 36: Position control - ramp input signal | 43 |
| Figure 37: Position control - ramp input signal (zoom)..... | 43 |
| Figure 38: Position control - sinusoid input signal | 44 |
| Figure 39: Position control - sinusoid input signal (zoom)..... | 44 |
| Figure 40: Position trajectory – ramp input signal – PID controller..... | 46 |
| Figure 41: Position trajectory – ramp input signal – PID controller (zoom)..... | 46 |
| Figure 42: Constant position of the punch and random env. force – PID controller...47 | |
| Figure 43: Constant position of the punch and random env. force – PID controller...48 | |
| Figure 44: trajectory – ramp input signal – FLC controller..... | 49 |
| Figure 45: trajectory – ramp input signal – FLC controller (zoom) | 49 |
| Figure 46: Constant position of the punch and random env. force – FLC controller ..50 | |
| Figure 47: Constant position of the punch and random env. force – FLC controller ..51 | |
| Figure 48: Position trajectory – ramp input signal – PID v FLC - experiment | 52 |
| Figure 49: Position trajectory – ramp input signal – PID v FLC - simulation..... | 52 |
| Figure 50: Position trajectory – ramp input signal – PID v FLC - experiment | 53 |
| Figure 51: Position trajectory – ramp input signal – PID v FLC – exp. (zoom) | 53 |
| Figure 52: Position trajectory – sinusoid input signal – PID v FLC – experiment..... | 54 |
| Figure 53: Position trajectory – sinusoid input signal – PID v FLC – exp. (zoom) | 54 |
| Figure 54: Position trajectory – sinusoid input signal – PID v FLC - experiment | 55 |
| Figure 55: Hydraulic pressure in chamber A and B - exp. v sim. - PID controller | 55 |

Thesis overview

Hydraulic systems find an application in constantly increasing number of situations. To encounter new challenges modern control laws have to be employ. A short history of hydraulic systems, as well as a review of current areas of application and control techniques used in fluid power systems, is first presented. This thesis focuses on the situation when hydraulic system has to interact with the environment. A position-based impedance controller is proposed and demonstrated on an existing hydraulic press with a proportional solenoid actuated servo-valve and a two-way, vertically mounted hydraulic cylinder. A proportional-integral-derivative (PID) controller and Fuzzy Logic Controller (FLC) are primarily developed to meet the accurate positioning requirements of the impedance control formulation. The impedance filter, placed in force-feedback loop, modify a desired trajectory of the hydraulic actuator according to a specified behavior. The modified trajectory is fed to the position controller and control signal is sent to the proportional valve.

Simultaneously with the experiment conducted on the real hydraulic press, impedance control was performed in computer simulation. To represent actual hydraulic system during the simulation a non-linear model of the whole hydraulic system (cylinder + servo solenoid valve) developed by Ferreira in [Ferreira02] was parameterized with the use of data sheet and experimental values. The model reproduces both static (pressure and flow gain and leakage flow rate) and dynamic (frequency response) characteristics of the real valve. Computer simulation was conducted in Matlab/Simulink[®] environment.

Experiments were carried out in free space and in environmental contact, using two different position controllers. The tests show the effectiveness of the proposed approach in both situations, as well as in non-contact/contact transition. Simulations results are presented and good performance of the non-linear model is obtained. Finally, the experimental and computer simulation results are compared and discussed. Also ideas and propositions for future work are given.

Chapter 1 Introduction

1.1. History

1.1.1. Hydraulic systems – characteristics

Hydraulic systems have been present in heavy machinery and industrial manufacturing since a very long time. During these years they were constantly modifying, changing and improving. Starting as simple hydro-mechanical devices became sophisticated electro-hydraulic systems controlled by microprocessors. Hydraulic systems found an application in all situations where large forces are needed or high loads are encountered. Good ratio between force and torque delivered and the actuator weight and size is the main advantage of fluid power and reason for its popularity. Moreover hydraulic actuators have higher speed of response than other types of machines (e.g., electrically driven) and can be operated under different conditions (e.g., continuous, reversing). Due to the higher bandwidth than electrical motors, fluid power systems found the application when high oscillations, fast start, stop or reversal is required [Durfee09].

Initially used for open loop actuation, hydraulic systems have been developing and by using servo-control techniques, which allow accurate closed loop motion control, increased the number of their applications [Kroll02]. Constant development of computer power and electronic components as well as high performance of proportional valve and increase of the quality of mechanical components allow applying modern control laws in complex hydraulic systems and extend their application to areas where electro-mechanical servo-systems have dominated. While an electrical power system is usually complicated containing breaks, transmissions and wide variety of other components, hydraulic power systems to achieve the same effect needs only a pump, a valve and a cylinder. This simplicity is another reason for popularity of these systems.

Features like relatively quick response times (see Figure1, [Dorf95]), as well as ability to produce large forces and high durability, connected with lower cost causes that hydraulic systems became, in many applications, a good alternative for electrical motors.

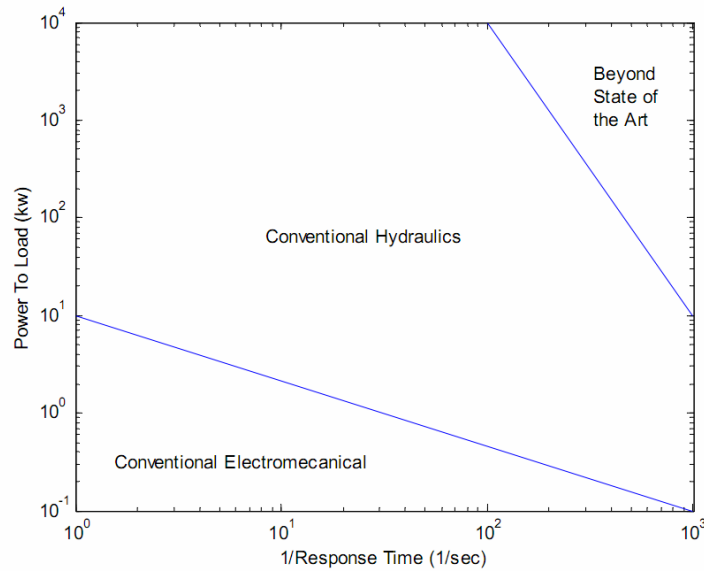


Figure 1: Comparison of electromechanical and hydraulic system response times

Besides unquestionable advantages of fluid power, there are also disadvantages. The main problems connected with hydraulic power systems are complex dynamics and non-linearities, which cause the parameterization of the controller, as well as testing of new control algorithms very difficult [Ferreira04]. Sources of these nonlinearities can be found in the features of the fluid power chain, such as the compressibility of the hydraulic fluid, friction in the hydraulic cylinder and the complex properties of the controller valves. These features create restrictions in range of application of hydraulic actuators, especially in the situation where high performance is required. Due to some undesirable characteristics usage of hydraulic actuators in high precision machines and robotics systems in the factory environment, is difficult.

Emergence of new technologies as well as constant development of already existed extends significantly the range of application of hydraulic systems. From huge machines like hydraulic presses through industrial robots to small hydraulic micro-drives, hydraulic systems are constantly increasing possibility of their applications.

Hydraulic systems are commonly used in situations where relatively large forces or torque are required like industrial presses (e.g.: 40.000-ton Forging Press in an aerospace company Shultz Steel), excavators used in construction industry for large digging and lifting operations (e.g.: Caterpillar 345 CL with digging force 60.200 Lbs) or materials transport machines (e.g.: Caterpillar 7673- the largest mining truck in the world) [Durfee09]. Industry which widely uses hydraulic systems is automobile industry (braking, steering, active suspension systems) [Alleyne95], not to mention also aerospace industry (landing gears). Other applications of hydraulic solutions are all kinds of simulators where fast and stiff response of resisting loads is required: driving simulators [Gardner95], flight simulators [Mayer92] as well as simulators used by civil engineers to test civil engineering structures and their behavior during earthquakes (e.g.: The MAST System at the University of Minnesota) [French04]. In opposition to designed production lines dominated by electrically powered robots, mobile robots intended to conquer rough and inhospitable terrain use hydraulic solution [Cubero00]. Off-shore engineering uses almost only hydraulic actuators - teleoperated from on board a surface ship - because of their robustness and good power-weight relation [Clegg00]. For the same reasons fluid power is used in logging machines to cut trees in place [Robinson01] as well as in hydraulic cutters or spreaders mainly used by emergency rescue to cut crashed vehicles. Also agriculture found many applications for hydraulic systems from agricultural harvesters [Stroup81] to cotton pickers [Brandt86]. It is necessary to mention their usage in industrial environment, where hydraulic systems play more and more important role, constantly increasing their range of applications, becoming important supplement for electrical robots.

1.1.2. Control of Hydraulic Systems

Almost 150 years after Pascal described the principles of hydraulic fluids (role that pressure is transmitted equally in all directions), Josef Bramah constructed and patented first hydraulic press, using water as a transmission medium [Bramah95]. It was the beginning of permanent and steady process of development of hydraulic systems, which during these years evaluated from simple, purely hydro-mechanical machines to very complicated, highly efficient systems, which combine knowledge not only of mechanical and hydraulic engineering but also electronic and control engineering. From the beginning control of fluid power became an important issue for all researchers, constructors and engineers. First hydraulic machines using pressurized water to drive processing machines like mills had an open loop control and were working without any electrical interface. In 1870 Brown used, for the first time, mechanical feedback to control the position of a valve-controlled cylinder in his ship steering system [Edge97]. War time created a demand for developing more sophisticated servo-control techniques, based on closed loop motion control for automatic fire control systems and military aircraft control. This progress was possible due to application of new materials, improvement of new transmission fluid and development of electronics, microprocessors and control technology.

First attempts to analyze and control of hydraulic systems- based on linear models- were not very precise, due to the high nonlinear nature of these systems. There were some endeavors like [Lin90], [Plummer96] to use linear control theory in description of nonlinear models, however they required complicated and detailed analysis of the system and were difficult to implement. Lin applied LQR theory based on the approximate solution of the system's periodic Riccati equation adding to the original system additional state to apply integral control. On the other hand Plummer used adaptive control together with linear control theory to compensate models nonlinearities.

Advances in other areas of research (electronic, microprocessors) enable to handle some uncertainties in modeling of the systems. As stated in [Burrows00]: "There is widespread interest in exploring the applicability of state feedback control, adaptive

control (self-tuning, model reference, gain scheduling), robust control (variable structure and H-infinity) and non-model-based control schemes (genetic algorithms, neural and fuzzy logic control).” Apart from control schemes listed by Burrows there is also the most common and well described PID control, linear quadratic numerical control (LQR), general and adaptive model predictive control (MPC) and of course combinations of different control schemes such as fuzzy-neural controllers. The implementation and application of these control methods in nonlinear hydraulic systems is the constant challenge for researchers and engineers.

In state feedback control signals from all system states feeding back the reference signal. In hydraulic system which has many uncertainties of the model and not all of the states are measurable, missing states have to be reconstructed. Optimal control schemes which are applied in this situation use linear quadratic Gaussian (LQG) design method [Friedland86]. The application of this method in controlling of the velocity of a hydrostatic transmission was described by Lennevi in [Lennevi95]. It has to be pointed out that LQG method is used to describe linear systems. That is why in case of non-linear hydraulic systems this method is optimal, only at a particular operating point.

One of the most common control schemes is PID controller. Depending on the controlled parameter, a structure of a controller can differ [Edge96]. PID controller can be implemented in electronic circuit as well as in software. The examples of application of PID control can be found in [Paoluzzi95] who used digital implementation of the controller to control the displacement of swashplate piston pump and in [McAllister95] where two PID controllers were used to maintain the center of a sample in a servo-hydraulic testing machine. In Chapter 4 more detailed description of PID control will be presented, together with its application in real system

Adaptive control is based on the assumption that controller parameters can be automatically adjusted to the operating conditions by using the knowledge of how the parameters affect behavior of the system- gain scheduling (example of an application of this scheme can be found in [Virtanen93]) or by employing a self-adaptive control

scheme. In case of self-adaptive control two approaches have been developed: self-tuning control and model reference adaptive control (MRAC).

Self-tuning control uses mathematical model of the plant to perform on-line parameter identification applying plant input-output data. Controllers parameters are updated by these identified plant parameters. This control scheme of hydraulic power system was investigated by Vaughan and Whiting in [Vaughan86] who applied pole placement method to a servo-hydraulic positioning system and showed that plant could adopt itself to the changes of supply pressure and still present a good performance. Plummer and Vaughan described robust adaptive control scheme with fast adaptation and with large tuning transients for electro hydraulic positioning system [Plummer96]. Also Daley [Daley87] and Wu and Lee in [Wu95] demonstrated an effectiveness of self-tuning control applied to hydraulic power systems.

Model reference adaptive control (MRAC) is similar to self tuning control but the identification of the plant is not required. Desired performance of the model is represented by the transfer function. The difference between this signal and the plant creates the model-following error which is used to adjust control scheme. Some applications of model reference adaptive control can be found in [Edge87], [Thollot95] or in [Egde95] who applied hybrid MRAC/sliding-mode control scheme to control two-axis hydraulically actuated robot manipulator.

The description of robust system is given by Dorf and Bishop in [Dorf95]: “The goal of robust systems design is retain assurance of system performance in spite of model inaccuracies and changes. A system is robust when the system has acceptable changes in performance due to model changes or inaccuracies.” Examples of robust controllers are variable structure control and H-infinity control. Application of sliding mode control (which is an example of variable structure control) in proportional-valve position control is described by Vaughan and Gamble in [Vaughan92]. Sliding mode scheme was also used by Becker in position control of hydraulic cylinder [Becker95] and by Habibi to control hydraulic industrial robot [Habibi91]. H-infinity control has not gained big popularity in fluid power application- although its good performance- due to the high-order controller transfer functions (e.g. [Piche91] and [Piche92]).

In situations when system is highly non-linear- like in case of hydraulic systems- it is useful to apply control schemes that do not require mathematical modeling. Two non-model-based control schemes which found wide application in control of hydraulic power are fuzzy logic control and neural control. General introduction to fuzzy logic control can be found in [Liu93] and some illustrative examples in [Klein95]. More detailed description of fuzzy logic controllers and its implementation in real system is given in Chapter 4.

Neural control also gives the possibility to avoid mathematical modeling while achieving non-linear robust control. Overview of some approaches to neural control is presented by Liu and Dransfield in [Liu93]. Similar experiments, however conducted independently, are reported in [Sanada93] and in [Newton95]. Both of them employed neural controller in valve-controlled hydraulic motor control system; however Newton used slightly more complex controller. Japanese experiment as well as the one conducted by Newton showed good performance of the system.

Except control schemes listed above that are applied in control of hydraulic systems there are also in use “hybrid control schemes”- combinations of these controllers. Niemela and Virvalo [Niemela95] proposed fuzzy state controller which combines fuzzy logic with classical state feedback control as an alternative for pure fuzzy logic controller applied in hydraulic servo-cylinder position control presented in [Shih93].

Application of position-based impedance control- which is also one of the hybrid control schemes- in control of hydraulic press will be presented in this work.

1.2. Impedance Control

Tasks performed by robotic manipulators can be divided into two types due to the interaction with environment. In a first case manipulator only follow a position trajectory in free space without coming in contact with its environment (e.g., arc welding or spray painting). In a second case, during the process, interaction between robotic manipulator and environment exists (e.g., assembly, drilling, or digging). While in first situation only position of the manipulator has to be controlled, in the second situation contact force has to be regulated. To ensure that force of the manipulator remains in a specific range and the task is performed correctly, two approaches are commonly used.

First solution is a hybrid force/position control. In this method task space is divided into degrees of freedom in which only on factor force or position is controlled. Calculation of the control torques is based on a dynamic model of a manipulator [Heinrichs96]. Literature contains variety of control algorithms, called “hybrid controls”, to simultaneous control of the force applied to constrain and position of robot’s tool.

Second approach commonly use is an impedance control. This solution is based on the assumptions that control of only one variable is not sufficient but instead of this dynamic relation between variables (the endpoint position and the environmental contact force) should be regulated. As Hogan described in his work [Hogan85] system can produce force in response to imposed position or position in response to imposed force. This relation between force and position is called impedance. The required accelerations of end-effector are calculated according to the desired impedance relationship. In both situations feedback loops at the manipulator joints are closed such that from the perspective of environment the robot appears as specified impedance (target impedance).

These two types of control are very similar and the difference between them is only in calculation of the desired accelerations. While for electrical driven manipulators the assumption that torques are controllable and acceleration can be compute from joint torques is not questionable in case of hydraulic actuators pose a difficult problem. These difficulties arise from the character of hydraulic power chain where actuator

torque is controlled by the control current in indirect way. Control current is used to control a movement of spool valve which enable the flow of hydraulic fluid into and out of the actuator. The actuator torque is proportional to the pressure differential buildup caused by the flow of the fluid. That is why there is always some delay introduced into the system [Heinrichs96].

Different strategies of implementation of impedance control have been developed. Position-based and force-based impedance controls are the most common. The force-based impedance controller is actually a force controller nested within position feedback loop. Desired force trajectory is modified by the information from position sensors. On the other hand in position-based impedance controller a position controller is placed inside force-feedback loop. Force feedback is used in to modify the desired position of end-effector. As stated in [Salcudean97] position-based impedance control is a mechanism that softens a stiff position source using contact force information while force-based impedance control can be viewed as a mechanism that stiffens a soft force source. This implementation required neither dynamic model of the robot nor the model of environment, which simplify the control.

The main reason why impedance control has been developed was to enable highly non-linear hydraulic manipulators to interact with the environment. First practical application of position-based impedance control scheme to control hydraulically actuated industrial manipulator is presented in [Heinrichs95]. Controller showed good static force control ability and very good performance in dynamic tasks such as impact force reduction. Also Ferretti in [Ferretti04] studied application of impedance control; however his attention was focused on industrial manipulators with elastic joints. Salcudean and Tafazoli developed position-based impedance controller for excavator-type manipulators [Salcudean97].

1.3. Organization

The thesis is organized into 6 chapters:

Chapter 1, Introduction, contains a brief introduction to the field of hydraulics and controllers, an overview of robot control research and various approaches that have been proposed in the context of hydraulic systems.

Chapter 2, Experimental Test Platforms, contains a description and familiarization of the actual experimental test platform, a prototype hydraulic press, as well as the control system hardware and software to be utilized.

Chapter 3, Modeling of the system, contains the description and familiarization of the nonlinear computer models of the hydraulic valve and cylinder, as well as the results of parameterization of the model.

Chapter 4, Implementation of Impedance Controller, contains the description of implementation of impedance controller in the real system as well in computer simulation. In the third section of this chapter the description of the controllers used for position control (PID Controller and Fuzzy Logic Controller) is presented.

Chapter 5, Experimental Results, presents the results of the experiments conducted for two different controllers (PID Controller and Fuzzy Logic Controller) and also the comparison of the results from the computer simulation and from real experiments.

Chapter 6, summarizes the work presented and draws relevant conclusions, as well as discusses future work that could be done.

Chapter 2 Experimental Test Platform

2.1. Hardware

The actual experiment was conducted with the use of 100kN hydraulic actuated press located in the Department of Mechanical Engineering at University of Aveiro, designed to perform aluminum stamping operations and mechanical tests. The press has two hydraulic servomechanisms. First hydraulic cylinder, driven by a servo-solenoid flow control valve, supports the punch tool. Second hydraulic cylinder, where the chamber pressure is controlled by a servo-solenoid pressure control valve; supports the operations of loading and unloading of the press blank holder. The hydraulic press is presented in Figure 2. Figure 3 and 4 show upper and lower cylinders, proportional valves and position sensors.



Figure 2: Picture of Hydraulic Press



Figure 3: (left) Upper cylinder, valve, load cell and position sensor



Figure 4: (right) Lower cylinder and valve

Upper cylinder used to actuate the punch tool is a Bosch-Rexroth® servo cylinder with 80mm piston diameter and a range of motion of 200mm. This cylinder has low friction hydrodynamic seals to improve dynamic performance. Valves were selected to control the hydraulic actuators of the system by proportional inputs and provide high-speed response and good precision of the operations. The motion control of the punch tool is performed using a Bosch-Rexroth® servo-solenoid valve; model NG6 OBE with integrated electronics, which has a functional bandwidth of 120 Hz for inputs of $\pm 5\%$ of the maximum valve input signal. Lower cylinder is driven by a servo-solenoid pressure control valve from Bosch-Rexroth, also with integrated electronics, with the aim of better control the blank holder force. A variable displacement axial piston pump, model PVQ10 from Vickers®, along with a 5dm³ capacity accumulator, model IVH 5-330 from OLAER® provides to the system hydraulic power at a constant pressure. The hydraulic system is able to generate the pressure up to 200bar which gives the maximum punch force approximately 100KN. The overall hydraulic circuit implemented to operate the press is shown in Figure 5.

2.3. Data Acquisition and Control

Data acquisition and control of the press are done with the use of a real time DSP based control card, model DS1102 from dSPACE[®]. The setup and connection of the data card is showed in Figure 6.

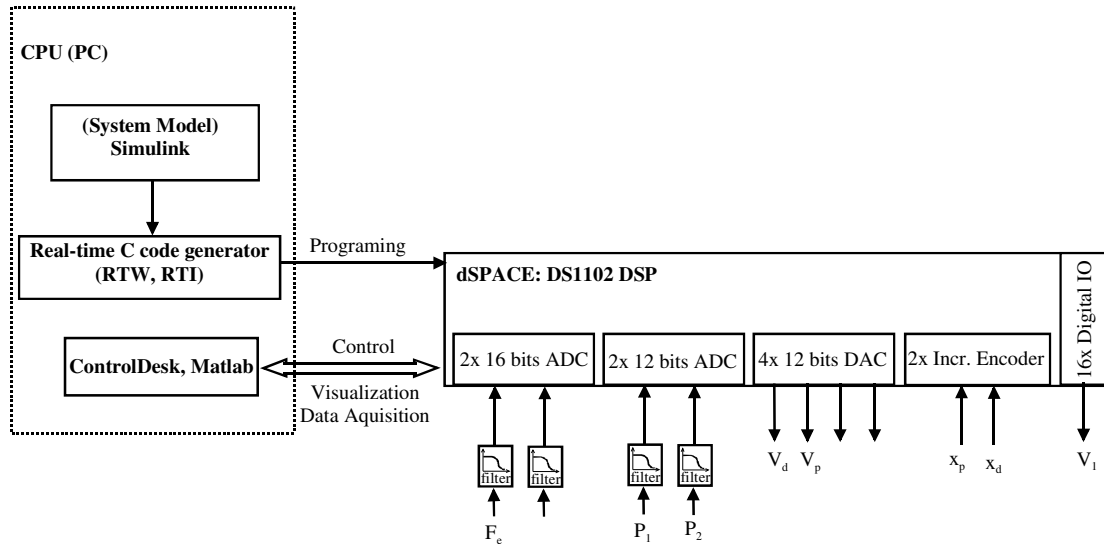


Figure 6: DS1102 DSP Comp. Card setup for data acquisition and control

The dSPACE DS1102 computer card has two 16 bit and two 12 bit analogical input channels, four 12 bit analogical output channels, sixteen digital I/O channels and two inputs for incremental encoders.

The control and operation of the press are accomplished by the use of the computer card in conjunction with the Matlab/Simulink[®] platform. This hardware/software setup enables the simultaneous monitoring and acquisition of data as well as changes of control parameters and press operations in real time. Software to control, operate and monitoring the hydraulic press is implemented in the Matlab/Simulink environment. Real-Time Workshop (RTW) generates, from Simulink[®] models, ANSI C code automatically, optimized for execution in real time. RTW complemented by the Real Time Interface (RTI), from dSPACE, enables compilation of the ANSI C code generated by RTW, the incorporation of dSPACE functions and loading of the executable program to the real time hardware. Update of parameters and monitoring of variables is possible also through the Matlab (the MLIB/MTRACE library), by

using a file with the references of the parameters and signals used in the Simulink model generated by RTI. Interaction with the real time application can be done also with the use of *ControlDesk* delivered by dSPACE. These application supplies programmers with the set of tools (predefined virtual instruments) that allows the fast development of interfaces for experiments using drag&drop mechanisms. Simulink® model to perform position-based impedance control is presented in Chapter 4.

The control interface was created with the use of *ControlDesk* because the setup of Graphical User Interface (GUI) is simple and intuitive. It enables simultaneous monitoring of the performance and acquisition of data as well as changes of various control parameters in real time. The interface which was used to perform position-based impedance control of hydraulic press is presented in Figure 7.

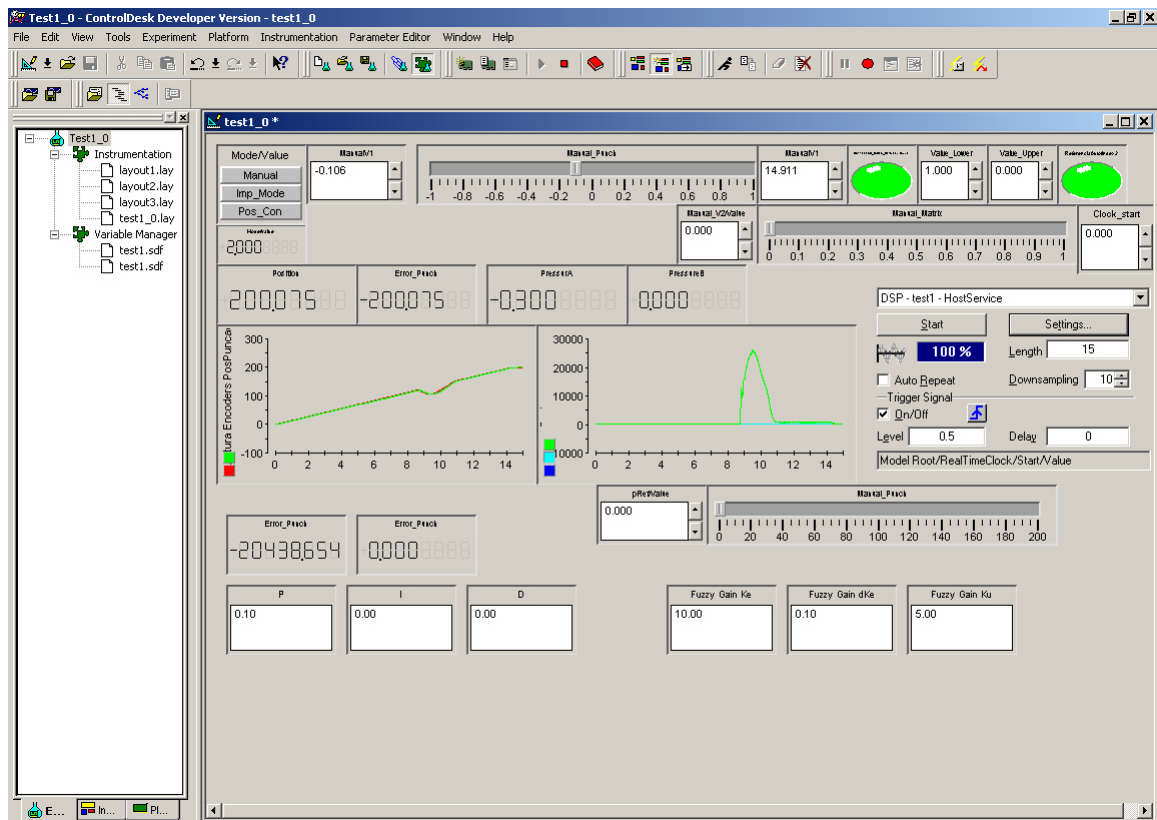


Figure 7: *ControlDesk* graphical user interface for impedance control

Chapter 3 Modeling of the System

3.1 Nonlinear Model

Development of electronics, microprocessors, high-power computers and engineering software, connected with a fall of prices of components created the possibility for building complex models of hydraulic systems for computer simulations. With the use of real-time simulator, controller can be optimized and tested without being connected to the real equipment. This solution reduces costs and increases the safety of the sensitive and expensive equipment, which could be damaged in case of undesirable behavior of the controlled system. Simulation can be accomplished on a normal PC in laboratory or office environment.

Building a computer model of hydraulic systems creates number of problems due to the complex and highly nonlinear dynamic behavior of these systems. The overall stiffness of the model that requires extremely small step size connected with model complexity demands usage of high performance computer hardware. Application of semi-empirical model instead of pure physical model can reduce model complexity and lower the costs of simulation. Capturing only the most important characteristics of the system behavior is sufficient to design the control system. Semi-empirical models can be tuned and parameterized using data supplied by manufacturer or experimentally measured characteristic curves and requires less computer power.

An appropriate nonlinear model of hydraulic actuator has been developed by Ferreira in [Ferreira04]. This work presents two complementary modeling approaches: semi-empirical model to model proportional valve and hybrid statechart to model the hydraulic cylinder. The paper describes the development of the semi-empirical models of valve spool dynamics and volumetric flowrate as well as models of cylinder piston dynamics, effect of bulk modulus and seal friction forces. The overall behavior of the cylinder model is described with a hybrid statechart.

All models mentioned above were joined together in a Simulink block diagram model. Each of them represents different operational aspect of the hydraulic press.

Simulink block diagram contains models of the control valve, dynamics and forces generated inside the cylinder as well as friction forces. All parameters were optimized to fit the model to the real hydraulic press behavior.

3.1.1. Valve Model

Valve is probably, due to its complexity, the most difficult part of hydraulic chain to model. Some researchers argue that because of faster dynamics than hydraulic actuators, model of the valve do not have to be included in the general model of nonlinear hydraulic systems. However to achieve high precision model and accurate control, model of the valve's dynamics has to be created. In this work modeling of the dynamics of the valve was done using second order transfer function.

While modeling, the dynamic part of the model can be separated from the static part, so the valve model can be divided into two main blocks with a serial connection as showed in Figure 8.

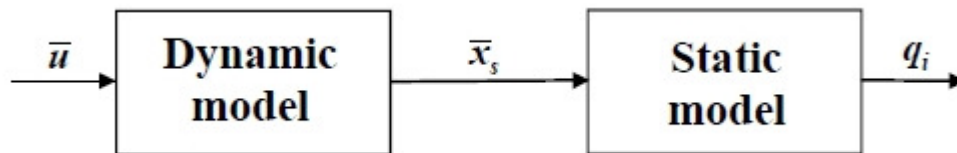


Figure 8: Division of the valve model (dynamic model and static model).

The first block represents non-linear spool position dynamics. The input of the block is an electrical, reference signal spool positions $\bar{u} \in [-1,1]$ and the output, the actual spool position $\bar{x}_s \in [-1,1]$. The second block characterizes the static behavior of the valve and models the port pressures q_i , according to volumetric flowrate related to the input spool position.

3.1.1.1. Dynamic Model – Spool Motion

Modeling of the valve spool dynamics was accomplished using second-order transfer function. Efficacy of this method was proved before by Quintas in [Quintas99] who analyzed a standard spring/mass/dashpot system with one degree of freedom to create

second order transfer function. The second order model suggested by Quintas is shown in Figure 9.

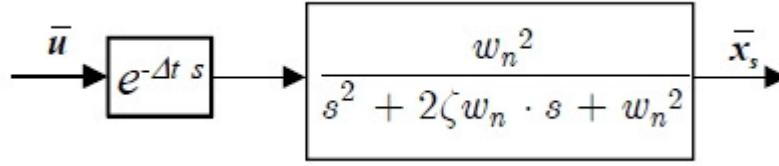


Figure 9: 2nd order model with delay to compensate the phase [Quintas99].

where \bar{x}_s is the position of the mass (valve spool), \bar{u} is the control signal applied to the valve (the input), ξ is the damping ratio associated with spool movement and ω_n the natural frequency of the spool.

On account of the application of the model in control simulation, frequency response of the spool position is the most important behavior to be modeled. Figure 10 presents a typical Bode diagram, provided by the producer, for a proportional valve Bosch-Rexroth[®], model NG6 OBE.

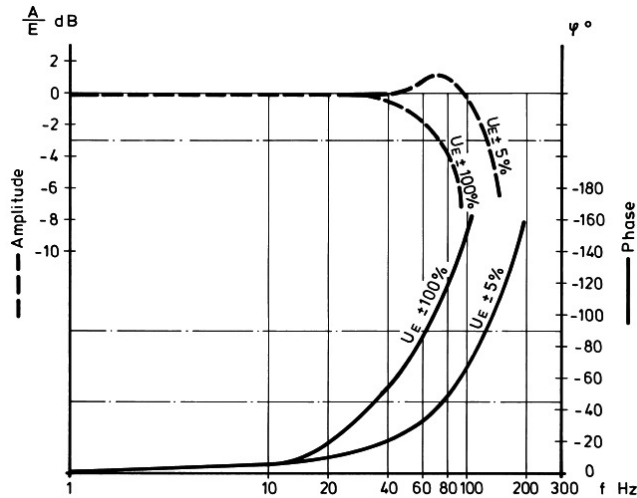


Figure 10: Bode plot of response for $\pm 5\%$ and 100% of valve spool range.

The optimization process showed the need of reducing the valve response to large control signal variations. This problem was solved by applying the method presented by Beater in [Beater98] that suggests introduction of nonlinearity into the model to restrict valve spool velocity. Desired frequency response was reached by introducing two nonlinearities to the model: saturation of valve's spool velocity (L_v) and saturation of valve's spool acceleration (L_a). The second order Simulink model with both saturations blocks is presented in the Figure 11. Due to a small hysteresis of the

valve (less than 1%) and by using spool position close loop some disturbances like the spool friction or the flow forces can be minimized.

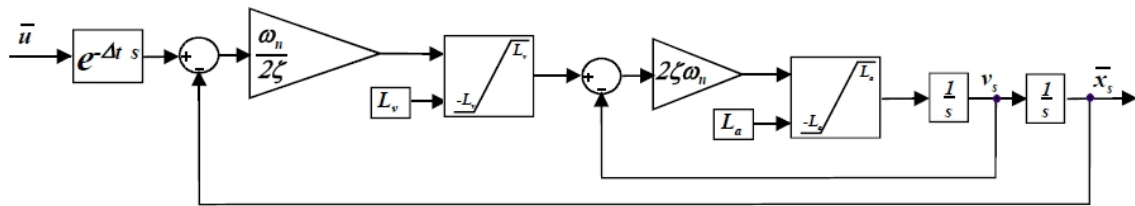


Figure 11: Block diagram of control valve dynamic model [Ferreira03].

3.1.1.2. Static Model - Volumetric Flowrate Model

Valve characteristics such as the pressure gain, leakage flow or flow gain can be considered as static as they occur mostly near the central spool position. Static valve model proposed by Ferreira in [Ferreira02] to calculate flow characteristics is similar to the model described in [Quintas99] and uses pseudo section functions $A_{ij}(x_s)$ to model the orifice areas versus relative spool position \bar{x}_s . Ferreira considered the valve (Figure 12) in which spool position modulates four control sections. The volumetric flow rate is considered turbulent the laminar flow being implicitly modeled in the pseudo-sections functions.

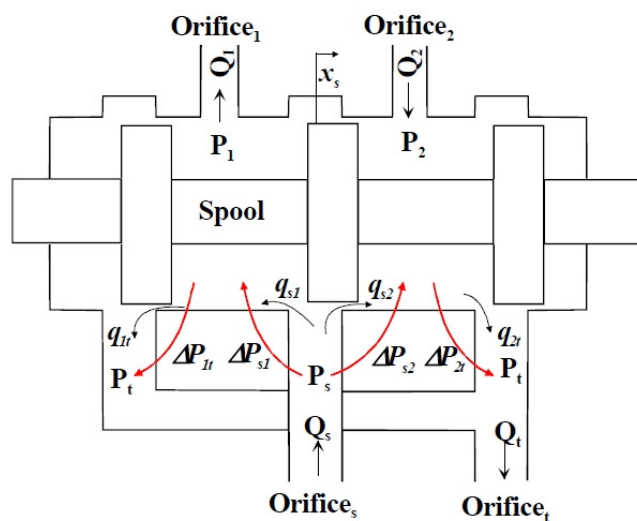


Figure 12: Diagram of controlled valve

For the pseudo section function $A_{ij}(x_s)$ the volumetric flow rate q_{ij} can be written as:

$$q_{ij} = \text{sign}(\Delta P_{ij}) \cdot A_{ij}(\bar{x}_s) \cdot \sqrt{|\Delta P_{ij}|} \quad (1)$$

Where $\Delta P_{ij} = P_i - P_j$ is the pressure drop between the two ports and $\text{sign}(\Delta P_{ij})$ is the sign of $(P_i - P_j)$.

In case of the valve presented in Figure 10, valve flow rate can be described by a set of four equations:

$$\begin{cases} q_{s1} = \text{sign}(\Delta P_{s1}) \cdot A_p(\bar{x}_s) \cdot \sqrt{|\Delta P_{s1}|} \\ q_{s2} = \text{sign}(\Delta P_{s2}) \cdot A_n(\bar{x}_s) \cdot \sqrt{|\Delta P_{s2}|} \\ q_{1t} = \text{sign}(\Delta P_{1t}) \cdot A_n(\bar{x}_s) \cdot \sqrt{|\Delta P_{1t}|} \\ q_{2t} = \text{sign}(\Delta P_{2t}) \cdot A_p(\bar{x}_s) \cdot \sqrt{|\Delta P_{2t}|} \end{cases} \quad (2)$$

High performance proportional valves have usually matched and symmetrical control orifices which gives the maximum loop gain, load stiffness and can reduce the number of different pseudo section functions. The valve has matched orifices if $A_{s1}(\bar{x}_s) = A_{2t}(\bar{x}_s) = A_p(\bar{x}_s)$ and $A_{s2}(\bar{x}_s) = A_{1t}(\bar{x}_s) = A_n(\bar{x}_s)$.

The valve is considered to be symmetrical if $A_p(\bar{x}_s) = A_n(-\bar{x}_s)$.

These pseudo section functions were implemented with hyperbolic functions. This method gives the possibility of analyzing two well-defined asymptotes. For a symmetrical and matched valve the hyperbolic functions can be described by equations:

$$\begin{aligned} A_n(\bar{x}_0) &= k_1 \cdot \bar{x} + k_2 + \sqrt{k_3 \cdot \bar{x}_s^2 + k_4 \cdot \bar{x}_s + k_5} \\ A_p(\bar{x}_0) &= -k_1 \cdot \bar{x} + k_2 + \sqrt{k_3 \cdot \bar{x}_s^2 - k_4 \cdot \bar{x}_s + k_5} \end{aligned} \quad (3)$$

Where $k_i \in \Re$ and $\bar{x}_s \in [-1,1]$.

The tank flow Q_t , source flow Q_s and outlet flows Q_1 and Q_2 may be formulated as follows:

$$\begin{aligned}
Q_t &= q_{1t} + q_{2t} \\
Q_s &= q_{s1} + q_{s2} \\
Q_1 &= q_{s1} - q_{1t} \\
Q_2 &= q_{2t} - q_{2s}
\end{aligned}
\tag{4}$$

3.1.2. Hydraulic Cylinder Model

The cylinder model presented below, developed by Ferreira in [Ferreira04] and used in this experiment contains mathematical models of the piston dynamics, the effective bulk modulus and seal friction force. Schematic diagram of the cylinder and valve is showed in Figure 13.

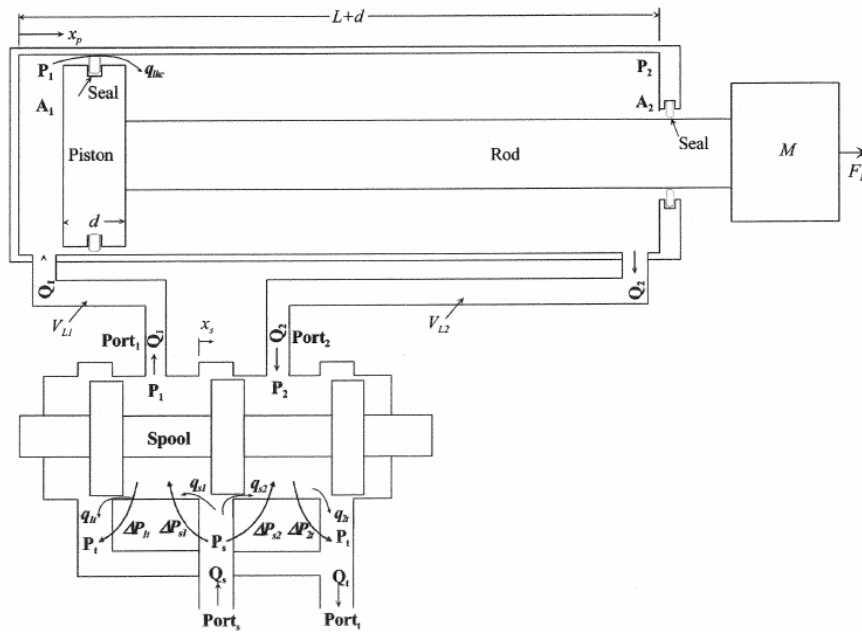


Figure 13: Diagram of control valve and hydraulic cylinder.

3.1.2.1. Piston dynamics

The continuity equation proposed in [Merrit67] was generalized by assuming isothermal conditions and with the use of the pressure-dependant effective bulk was formulated as:

$$\sum Q_{in} - \sum Q_{out} = \frac{dV_0}{dt} + \frac{V_0}{\beta(P)} \frac{dP}{dt}
\tag{5}$$

where V_0 is the control volume, $\beta(P)$ is the pressure-dependant effective bulk modulus, and P is the fluid pressure inside the control volume, Q_{in} and Q_{out} are the inlet and outlet flows. The cylinder chamber pressures were described by applying equation (5) to each cylinder chamber:

$$Q_1 = g_{lkc}(P_1 - P_2) + A_1 v_p + \frac{V_{L1} + A_1 x_p}{\beta_{e1}(P_1)} \frac{dP_1}{dt} \quad (6)$$

$$Q_2 = -g_{lkc}(P_1 - P_2) + A_2 v_p - \frac{V_{L2} + A_2(L - x_p)}{\beta_{e2}(P_2)} \frac{dP_2}{dt} \quad (7)$$

The flow in chamber 1 is expressed by the equation (6) and in chamber 2 by equation (7). V_{L1} and V_{L2} represent the line volumes plus the cylinder dead volumes. $\beta_{e1}(P_1)$ and $\beta_{e2}(P_2)$ are the pressure-dependant effective bulk moduli and represent the compressibility of the fluid, pipes and cylinder wells. Term $g_{lkc}(P_1 - P_2)$ describes cylinder's internal leakage flowrate, where g_{lkc} is the leakage conductance and P_1, P_2 are the pressures in chamber 1 and 2 respectively. The external leakage q_{lkc} is ignored.

Equations (8) and (9) show the piston velocity and the piston acceleration respectively:

$$v_p = \frac{dx_p}{dt} \quad (8)$$

$$a_p = \frac{dv_p}{dt} \quad (9)$$

The cylinder dynamics are defined by equation (10) as a sum of all forces that act in vertical direction.

$$Ma_p = P_1 A_1 - P_2 A_2 - Mg - F_f + F_L \quad (10)$$

where M is the total mass in motion (load, piston and rod), F_L is the total load force, F_f is the frictional force and g is the acceleration of gravity.

Equations (6) through (10) are implemented in the Simulink[®] model and by simultaneous calculations give immediately the actual position, velocity and acceleration of the cylinder. The friction is calculated utilizing a friction model and the hydraulic force is calculated using the differential pressures acting on each side of the internal piston.

3.1.2.2. Effective bulk modulus

In many simulations effective bulk modulus is considered as constant [Merritt67]. In case of hydraulic systems that have to operate in wide range of pressures, to receive satisfactory simulation results, a value of β_e has to be considered as pressure-dependant. The effective bulk modulus is defined for both cylinder chambers:

$$\beta_{e1} = \frac{10^5 + P_1}{BP_1 + C} \quad (11)$$

$$\beta_{e2} = \frac{10^5 + P_2}{BP_2 + C} \quad (12)$$

Where $B[P_a^{-1}]$ and C are constants related to the oil characteristics.

This model is based on a model proposed in [Yu94].

3.1.2.3. Friction model

Friction is one of the most important sources of non-linearities in hydraulic servo systems. Can cause a large steady state error and is an important factor that affects systems dynamics. In significant extent can decrease the force or torque available at the actuators. The source of friction in hydraulic cylinder is the force generated in the contact of the seals with cylinder walls. Friction differs depends on a velocity and motion state. Three types of friction can be distinguished in hydraulic systems: Stribeck friction, Coulomb friction, and viscous friction. As stated in [Ferreira04]: “for small velocities the hydraulic fluid acts as a superficial layer and the shear forces determine the friction. On the other hand, for high velocities and low pressures, a permanent fluid layer is developed and the friction is related to hydrodynamic effects. The friction than depends on the fluid viscosity characteristics and also on the

distribution of velocities along the fluid layer”. The need of motion controllers accelerates the development of suitable friction models. Initially static models of the friction were developed [Armstrong94]. Recently, due to the demand on analyzing high-accuracy servo-systems and development of friction compensators, dynamic models for friction were proposed, among others in [Swevers00] and [Tan01].

In this project, friction between the seal and the cylinder walls was modeled with the use of the LuGre dynamic model [Canudas95], which is the extension of the Dahl model [Dahl76]. This model defines a friction as a force generated by the contact of small bristles on the surfaces of two objects. In hydraulic cylinders bristle is represented by the seal (see Figure 14).

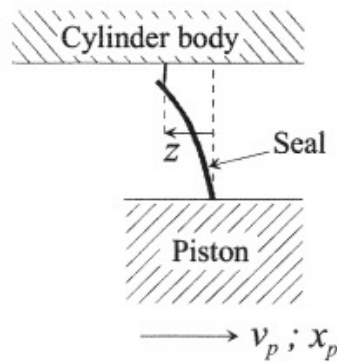


Figure 14: Diagram of the friction between seal and cylinder wall.

The average deformation of the seal is given as a state variable z and is defined by the equation (13) and where v_p is the piston velocity.

$$\frac{dz}{dt} = v_p - \frac{|v_p|}{g(v_p)} z \quad (13)$$

$g(v)$ is given by equation (14):

$$g(v_p) = \frac{1}{\sigma_0} \left[F_{CO} + (F_S - F_{CO}) e^{-(v_p/v_s)^2} \right] \quad (14)$$

where F_{CO} is the Coulomb friction force, F_S is the Stribeck friction force, v_s is the Stribeck velocity and σ_0 is the seal stiffness.

The friction force is considered proportional to the average deformation of the seal, piston velocity and depends on the average rate of deformation. The friction force is given by:

$$F_t = \sigma_0 z + \sigma_1 \frac{dz}{dt} + K_v v_p \quad (15)$$

where σ_1 is the damping factor of the seal motion and K_v is the viscous friction coefficient.

3.2 Parameterization

Nonlinear model created for the computer simulation has to be parameterized to adjust its performance to the behavior of the real system. Parameters are calculated on the basis of data supplied by manufacturer as well as experiments conducted on real system. Usually data sheet of the valve contains information like: load pressure characteristic (for null load flow), the nominal flow rate at the nominal pressure difference, an estimation of the flow gain near the origin and maximum leakage flow rate as well as Bode diagrams for different amplitudes of spool displacement (see Figure 8). Based on these information and using equation described in this chapter and presented earlier in [Ferreira02], the flow gain, pressure gain and leakage flow rate at the central spool position were calculated. The results are like follow: flow gain $\bar{K}_{q0} = 40 \text{ l/min}$, pressure gain $\bar{K}_{p0} = 64$, leakage flow $q_{lk} = 0.9 \text{ l/min}$, nominal flow rate $Q_n = 36 \text{ l/min}$, nominal pressure $P_n = 35 \text{ bar}$ and $P_s = 70 \text{ bar}$. Also parameters used in equation 3 to describe pseudo section functions were calculated:

$$K1 = -3.0785; \quad K2 = -0.099051; \quad K3 = 9.8403; \quad K4 = 0.2257; \quad K5 = 0.030665.$$

Parameters for friction model, calculated by Ferreira in [Ferreira03], are: $f_{c0} = 130N$

$$f_s = 110N, \quad v_s = 0.015 \frac{m}{s}, \quad k_v = 3000 \frac{N}{m}, \quad \sigma_0 = 5 \cdot 10^7 \frac{N}{m}, \quad \sigma_1 = 2000 \frac{N}{m}$$

To confirm that parameters were calculated correctly and that the model of the nonlinear hydraulic system has a good performance, two signals (step and sinusoid) were applied to the real system and to the model. Experiments were conducted in open loop. The setup for computer simulation is showed in Figure 15.

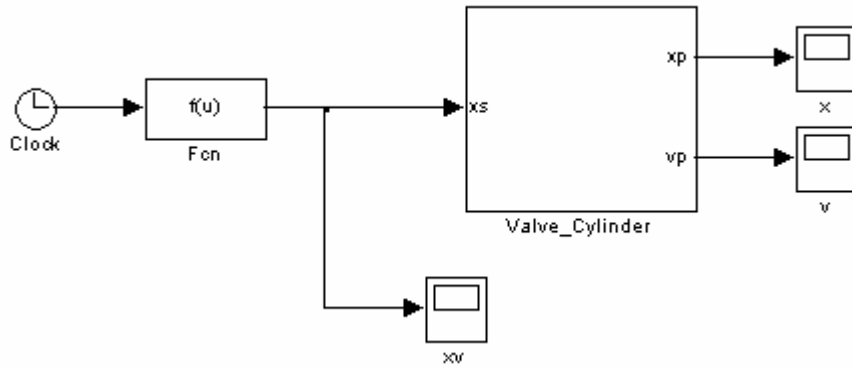


Figure 15: Simulink block diagram for simulation in open loop.

The response of the nonlinear model compared with the response of real system on the applied step signal can be seen in Figure 16 and on the sinusoidal signal in Figure 17.

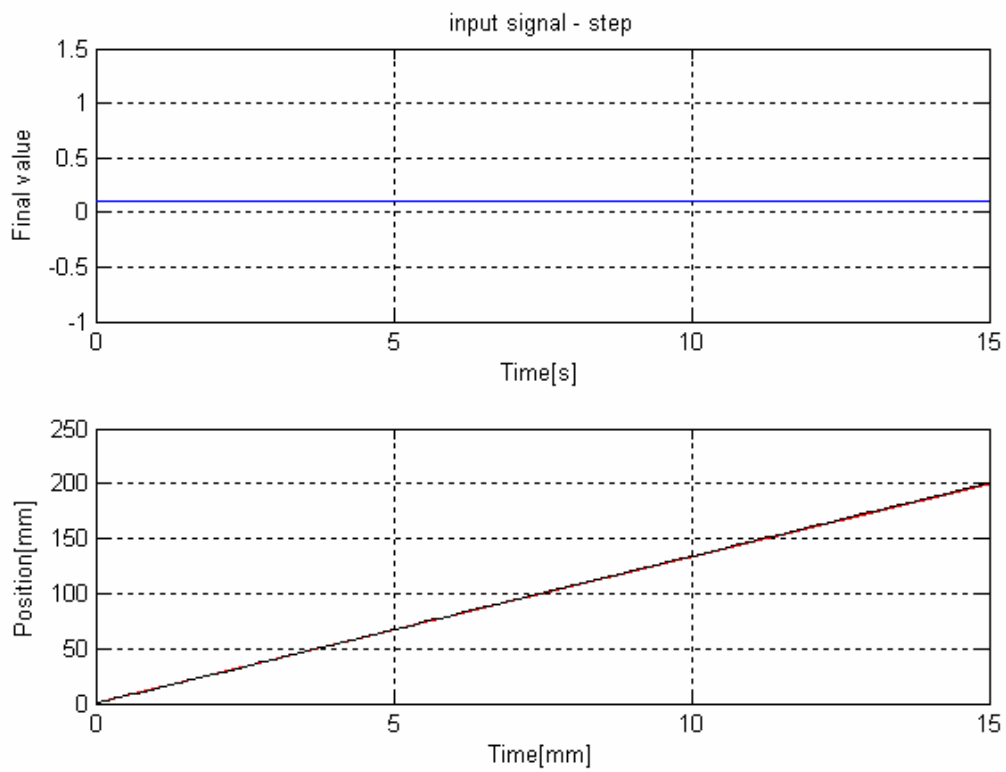


Figure 16: Model and real system response to the applied step signal

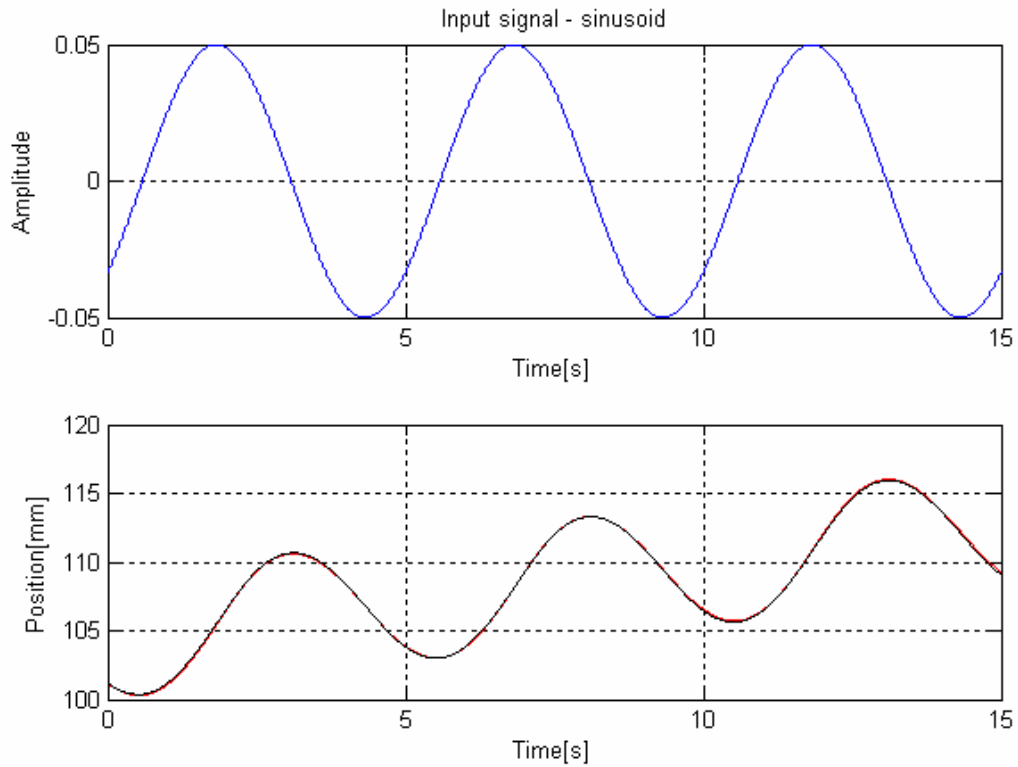


Figure 17: Model and real system response to the applied sinusoid signal

Experimental results show that parameters were calculated correctly. As can be seen in Figure 14 and Figure 15 both signals, the one received from the real system and the one received from the simulation, almost exactly match each other. It means that modeling method was correct and the nonlinear model, created to represent the real system, can be used in simulations.

Chapter 4 Implementation of the Impedance Controller

As it was described before, the main reason why impedance control has been developed was to enable highly non-linear hydraulic manipulators to interact with the environment. This method is based on assumption that dynamic relation between the endpoint position of the actuator and the environmental contact force should be regulated. Two the most common strategies of implementation of impedance control are position-based impedance control (see Figure 18) and force-based impedance control (see Figure 19). First method is based on a position controller placed inside force-feedback loop with impedance transfer function. Second method contains force controller nested within position feedback loop. In position-based impedance controller the desired position trajectory is modified by information about the force measured by load cell. In force-based impedance controller, information from position sensors influences on desired force trajectory.

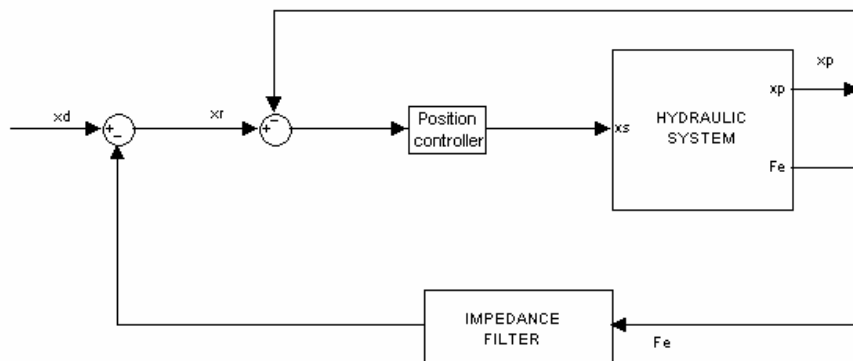


Figure 18: Position-based impedance controller

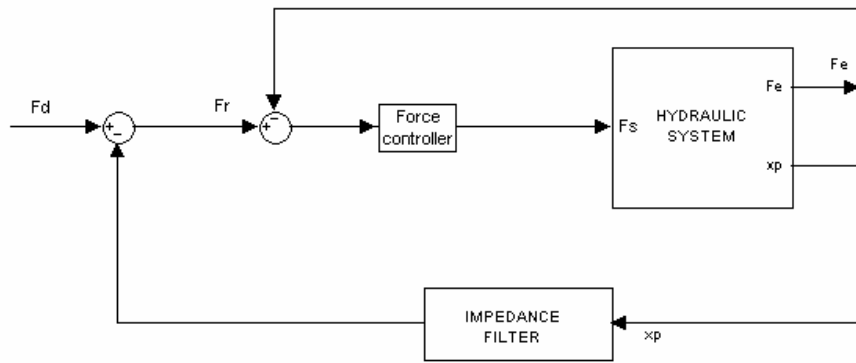


Figure 19: Force-based impedance controller

Implementation of position-based impedance controller, both in real system and in computer simulation, was presented in this work.

4.1. Real System

The Figure 20 demonstrates the Simulink model that was created to perform the position-based impedance control in real system. The model contains three operating modes: Manual, Position Control and Impedance Mode. Each of them was implemented to perform different task during the development of the controller. Manual Mode allows operator a manual control of the punch and blank holder by manual changes of the signal sent directly to the valves. This mode is used also to reset the optical position sensors and as a safety mode in situations of undesirable behavior of the press. Position Mode was implemented to perform optimization of position controllers used later in an experiment. To control position of the punch, two position controllers were proposed: PID and Fuzzy Logic controller (FLC). Both of them are described later in this chapter. Model contains a switch block that enables changes of the controllers in real time without rebuilding the Real Time Model. The reference position in this mode is constant. Proper mode to perform experiment is Impedance Mode. This mode contains controllers optimized before, the impedance loop to perform impedance control, reference position block (which in this experiment is a ramp or sinusoid) and real time clock.

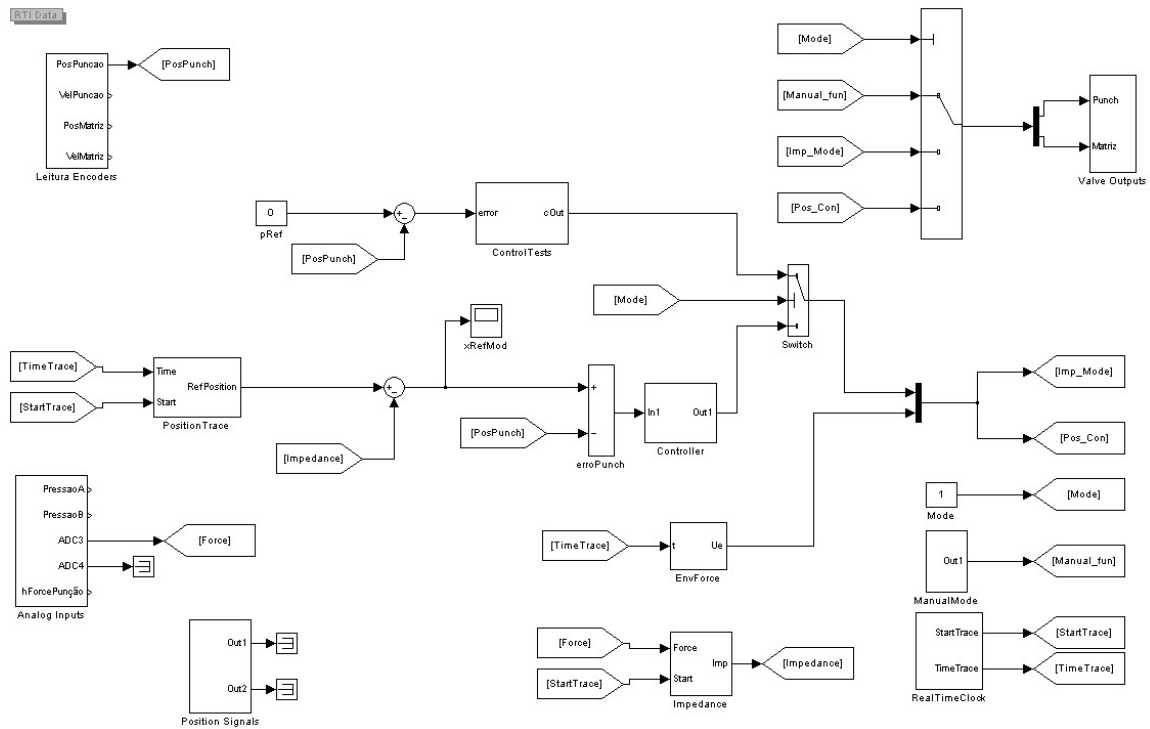


Figure 20: Simulink® block diagram for RTW with impedance controller.

The “Leitura Encoders” block receives the information about the actual position of the hydraulic actuator, measured by the position sensors, from the computer card. The difference between the reference and the actual position (the error) is passed to the controller block that in this experiment is the PID or Fuzzy Logic Controller. Simultaneously an external force that acts on the hydraulic actuator, measured by load cell mounted on the punch is passed through the impedance block that is a second-order transfer function and is subtracted from the reference signal. A control signal, calculated according to the desired impedance, is sent to the “Valve Outputs” block, which contains the software interface with the computer card and than to the control valve.

In this experiment the blank holder was used to simulate environmental contact force. The trajectory was implemented using two Look-up Tables: one to determine the trajectory and second to calculate the signal that is sent to the proportional valve.

Simulink model presented above was downloaded to the dSPACE card and the control interface for the experiment was created in *ControlDesk*. This application enabled changes of different model parameters in real time as well as simultaneous monitoring and acquisition of data. Figure 21 shows the interface created for the

optimization of the position controllers. Parameters of PID and FLC controllers could be changed by typing the values in the fields at the top of the interface (Fuzzy Logic Controller's parameters are marked by the red square) without the need of rebuilding Real Time Model. The changes of the behavior of the system could be observed directly on the graph and registered for further analysis. Interface presented below enables also the direct changes of the operating mode by pressing on of the buttons marked by blue square. At the bottom of the interface, marked by yellow square, there are fields to modify the parameters of the impedance in a force-feedback loop. Except the interface described here, two more interfaces were created for monitoring and modification of other parameters of the Simulink model.

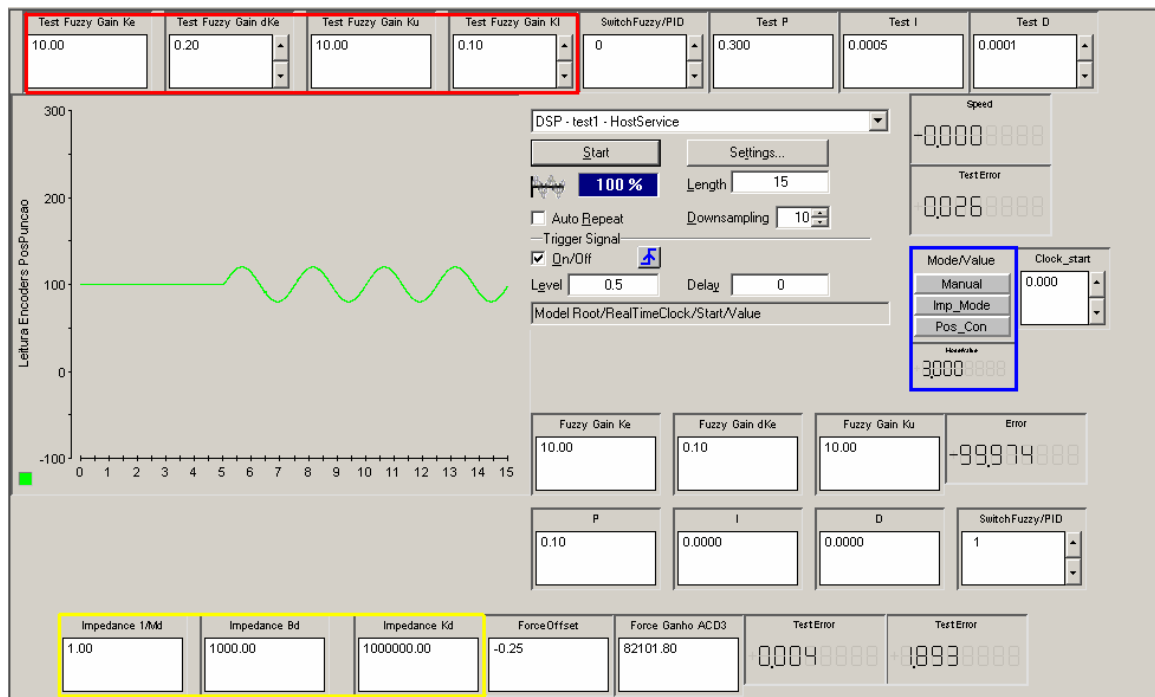


Figure 21: ControlDesk interface

4.2. Simulation

Figure 22 demonstrates the Simulink block diagram which was created to perform the position-based impedance control simulation on the computer in Matlab/Simulink environment.

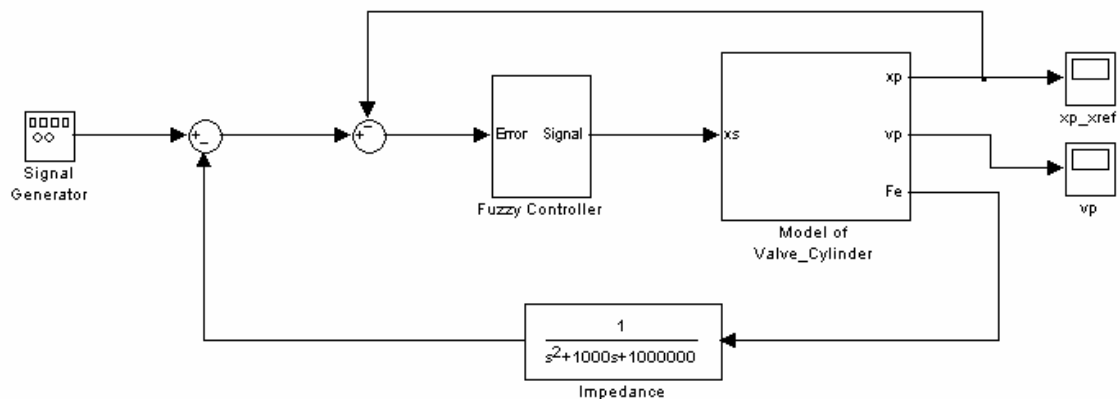


Figure 22: Simulink® block diagram with a model of hydr. system for simulation

To perform computer simulation, the model of the non-linear hydraulic system, represented by “Valve_Cylinder” block, was created and parameterized using the method and equations described in Chapter 3. This model enables the acquisition and monitoring of the reference position, the position simulated by the model, velocity of the piston as well as pressures in both chambers. To enable further comparison of the data acquired during the computer simulation with the results of the experiment, conducted with the use of real hydraulic press in laboratory, identical controllers (PID and Fuzzy Logic Controller) and transfer function were used both in above block diagram and in the real system.

4.3. Position Control

As it was said before position-based impedance controller is a position controller placed inside force-feedback loop with impedance transfer function. Kevin Edge in [Edge97] point out that whenever the performance of fluid power systems, controlled by different controllers, is compared usually “new” control schemes are compared against a fixed-gain classical PID scheme, despite its weakness in many high-performance applications. In spite of some disadvantages of PID control but due to its simplicity in implementation as well as big popularity, classical PID controller was used for position control in this experiment and compared with the performance of Fuzzy Logic Controller.

4.3.1. PID Controller

The classic PID (Proportional – Integral – Derivative) controller is a simple error-based feedback controller that corrects an error between a measured process variable and a desired reference signal. The controller calculates and sends to the system corrective action that can adjust the process and keep the error minimal. The Simulink block diagram of the feedback loop position control is shown below (see Figure 23).

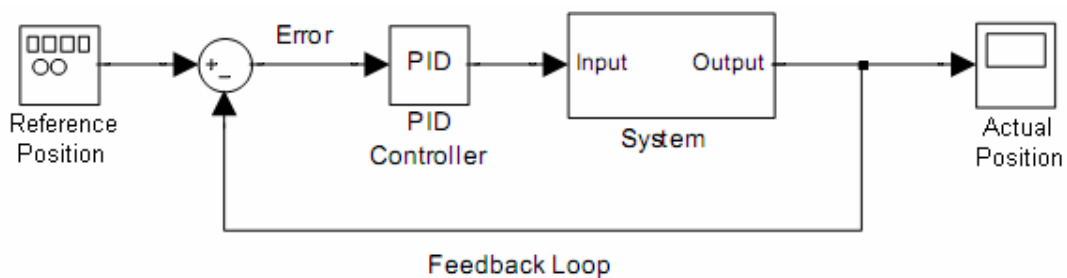


Figure 23: The Simulink® block diagram of the feedback loop position control

The PID Controller algorithm is based on three separate parameters: the proportional, the integral and derivative values. The proportional gain K_p determines the reaction to the current error and is applied directly between the set point (input) and the system output. A high proportional gain causes a large change in the output for a given change in the error. On the other hand a small gain results in a small output response to a large input error and makes the controller less sensitive. The integral gain K_i determines the reaction based on the sum of recent errors. By integrating the error, the

integral term gives accumulated error that was not corrected earlier and reduces the steady-state error of the system. The third parameter of PID Controller is the derivative gain K_d , which determines the reaction on the rate at which the error has been changing and is used to reduce overshoot caused by integral term. The Simulink block diagram model of the PID Controller is presented in Figure 24.

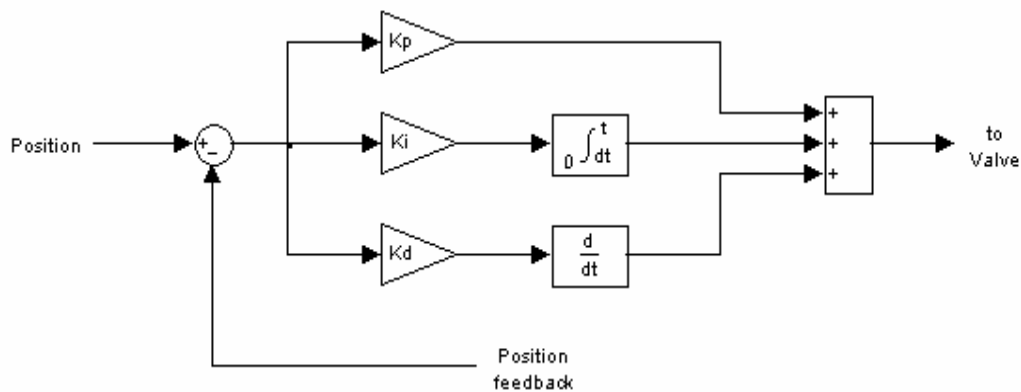


Figure 24: The Simulink® block diagram of PID scheme for position control

As stated in [Edge97]: “Because of valve non-linearities, it is possible that a steady state error will occur between the desired and actual positions. This will always occur when the actuator is a differential area cylinder or when a steady force has to be maintained. As a consequence, an integral-action controller may need to be employed as a means of minimizing steady state error.

4.3.2. Fuzzy Logic Controller

The biggest difficulty with model based control schemes is that their performance and effectiveness depends highly on the accuracy of the manipulator model. Traditional linear control methods, like PID control, require numerical model of the system, represented usually by linear transfer function. Numerical controller based on such model gives also linear results. In case of electro-hydraulic servo systems that are highly nonlinear phenomena, conventional linear controller can not get high performance. The transfer function is very often just rough approximation of the system. Moreover additional disturbances of the control can be caused by modeling error and uncertainties.

To overcome problems mentioned above Fuzzy Logic Controllers (FLC) can be applied. This control method was proposed for the first time in 1972 by Prof. L.A. Zadeh of the University of California at Berkeley [Zadeh72] and in 1975 Mamdani and Assilan applied fuzzy logic controller to the steam engine [Harris94]. A FLC is a model-free control scheme, where the control signal is calculated by fuzzy interface rather than from the system dynamics [Subuthi03]. By applying fuzzy set theory, logic reasoning of human beings can be simulated and mathematical control strategy can be translated into the linguistic control strategy. The most important part of the fuzzy controller is the set of linguistic fuzzy control rules and the engine to interpret these rules.

Fuzzy linguistic rules are usually expressed as a collection of simple if-then statements. In this experiment two input and one output controller was used, thus the fuzzy linguistic rule can be written:

R_i : IF X is A and Y is B , then Z is C

where R_i is the i th rule, X and Y are the states of the system output to be controlled, Z is the control input and A , B and C are the fuzzy linguistic values of the input and output universe of discourse. The IF part is called the "antecedent" and the THEN part is called the "consequent". Example of application FLC can be a car braking system, in this case one fuzzy linguistic rule can be formulated as follow: "IF X (brake temperature) IS A (warm) AND Y (speed) IS B (not very fast), THEN Z (brake pressure) IS C (slightly decreased)". As can be seen in this example, Fuzzy Logic Controller converts crisp mathematical input values to linguistic terms using membership functions, checks a rule base that produce a linguistic value to determine a suitable output and than again translate this linguistic output to an exact mathematical control signal. The process that uses fuzzy logic to formulate the mapping from a given input to an output is called fuzzy inference. Two main methods of implementing fuzzy inference are: Mamdani-type and Sugeno-type. The difference between these two types of fuzzy inference is in the way the outputs are determined [Mamdani75] [Sugeon85].

The whole process from acquiring data to producing a control signal by the FLC can be divided into three stages: Fuzzification, Reasoning and Defuzzification. The block diagram of this process is showed in Figure 25.

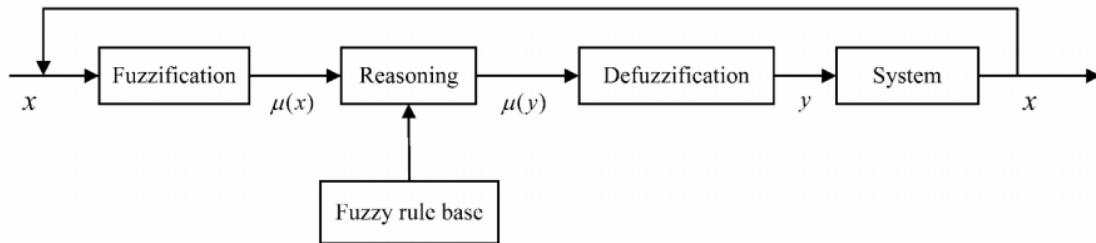


Figure 25: Architecture of the Fuzzy Logic Controller [Cho04].

4.3.2.1. Fuzzy Membership Function

Fuzzy membership functions are used to map the input parameter to membership grade that is always in a range from 0 to 1. The shape of the functions that was used in this controller is similar to the shape of Gaussian distribution with trapezoidal functions on the edges; however the shape of the membership functions is generally less important than the number of curves and their placement. For the good performance of the controller seven overlapping membership functions were defined, for each of the two inputs (see Figure 26 and Figure 27).

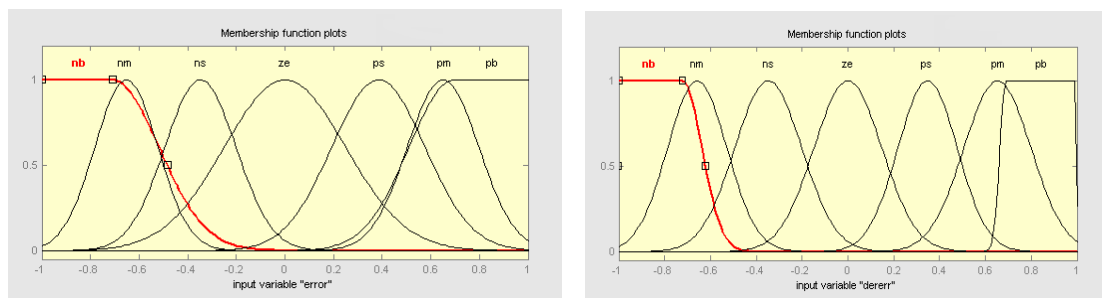


Figure 26: (right) Overall membership function plot for derivative of the error input

Figure 27: (left) Overall membership function plot for error input

Abbreviations above the curves mean: *nb* - Negative Big, *nm* – negative medium, *ns* – Negative Small, *ze* – Zero, *ps* – Positive Small, *pm* – Positive Medium, *pb* – positive Big.

4.3.2.2. Fuzzification

Fuzzification is a process in which the input values are converted into linguistic terms with the use of fuzzy membership functions. Input data are usually hard or crisp

measurements from some measuring equipment. In this experiment FLC was applied as a dynamic position controller in closed loop, thus the inputs are an error between the reference and the real position of the punch and derivative of this error.

During the fuzzification process input data are compared with the conditions of the rules to verify how the condition of each rule matches that particular input value. Fuzzified signal becomes a membership function to be evaluated. For instance if the position error was -0.1 , than it would belong to two membership functions: ns (negative small) and ze (zero) (see Figure 28). This signal would have negative small membership function value equal approximately 0.25 and zero membership value equal approximately 0.9 . Derivative of the error equal 0.2 would belong also to two membership functions: ze (zero) and ps (positive small) (see Figure 29). Values for both membership functions would be around 0.5 .

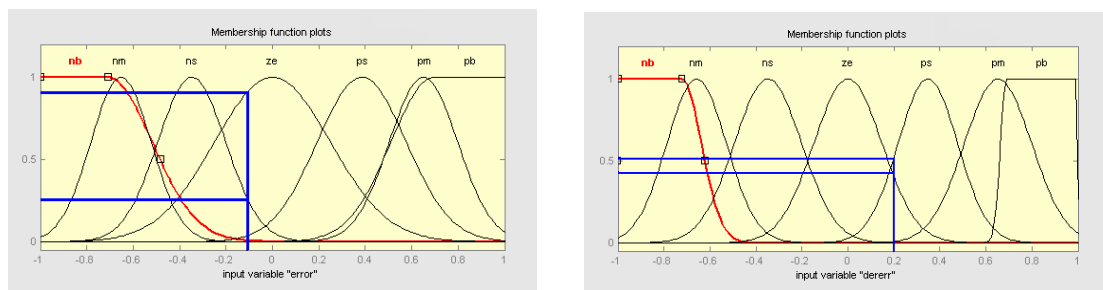


Figure 28: (left) Example of fuzzification for error = -0.1

Figure 29: (right) Example of fuzzification for derivative of the error = 0.2

4.3.2.3. Reasoning – fuzzy rule base

After the fuzzification process it is known how each part of the antecedent is satisfied for each rule. Forty-nine rules were generated for the controller, using seven membership functions for the error and seven for the derivative of the error. The rule base was created by combining every error membership function with each derivative of the error membership function. The rules are usually gathered in table as it is showed in Figure 30.

| | | Error (E) | | | | | | |
|------------------------------|----|---------------|----|----|----|----|----|----|
| | | NB | NM | NS | ZE | PS | PM | PB |
| Derivative of Error (dE) | PB | ZE | NS | NS | NM | NM | NB | NB |
| | PM | PS | ZE | NS | NS | NM | NM | NB |
| | PS | PS | PS | ZE | NS | NS | NM | NM |
| | ZE | PM | PS | PS | ZE | NS | NS | NM |
| | NS | PM | PM | PS | PS | ZE | NS | NS |
| | NM | PB | PM | PM | PS | PS | ZE | NS |
| | NB | PB | PB | PM | PM | PS | PS | ZE |

Figure 30: Fuzzy Logic Controller rule base

The aggregation process concludes individual rule based inference with a single output fuzzy set that is used thereafter for the calculation of crisp output value. This process takes place once for each output variable, just prior to the final step, defuzzification. Due to the commutativity of the aggregation process, the order in which the rules are executed is not important.

4.3.2.4. Defuzzification

The defuzzification is the last stage of the process and is opposite to the fuzzification. On this stage mapping is taking place from a space of the fuzzy control action into a space of the non-fuzzy (crisp) control action. In most cases the fuzzy set (the aggregate output fuzzy set) is converted to a number that can be sent to the process as a control signal. As it was said before the difference between Mamdani method and Sugeon method is in the way of defuzzification of aggregated information. In Mamdani method the output membership functions has to be fuzzy sets and based on these data the centroid of a two-dimensional function is found (see Figure 31). Mamdani-type of fuzzy inference is more general than Sugeon-type that uses, to produce the control signal, a pre-deffuzzified fuzzy set (the output of membership function is a single spike) and than calculates the weighted average of a few data points [Mamdani75] [Sugeon85]. Basically the Sugeno method can be used to model any inference system in which the output membership functions are either linear or constant.

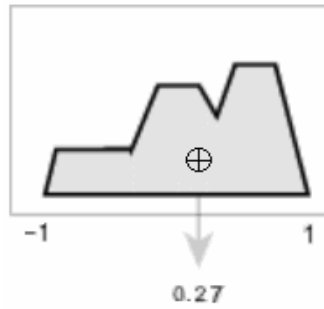


Figure 31: Centroid Defuzzification of the Result of Aggregation Process

4.3.2.5. Fuzzy Logic Control Surface

Fuzzy Logic Control Surface is a three dimensional visualization of the control signal over the whole input domain. Is generated based on the defined membership functions and the fuzzy rule base and in this case illustrates the control signal over the position error and derivative of the position error. FLC Surface is showed in Figure 32.

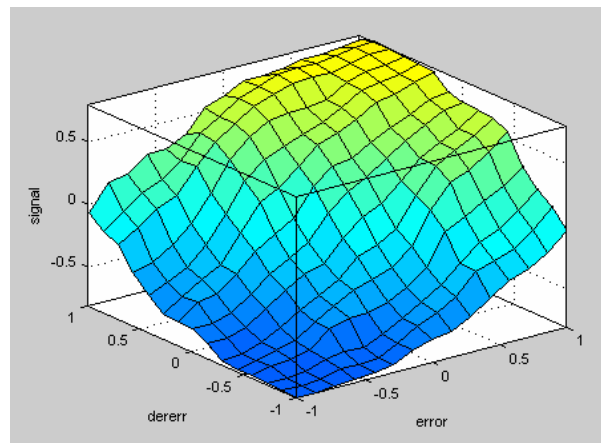


Figure 32: Fuzzy Logic Control Surface

4.3.2.6. Fuzzy Logic Controller in Simulink®

The Simulink block diagram showed below in Figure 33 was implemented to perform Fuzzy Logic Control.

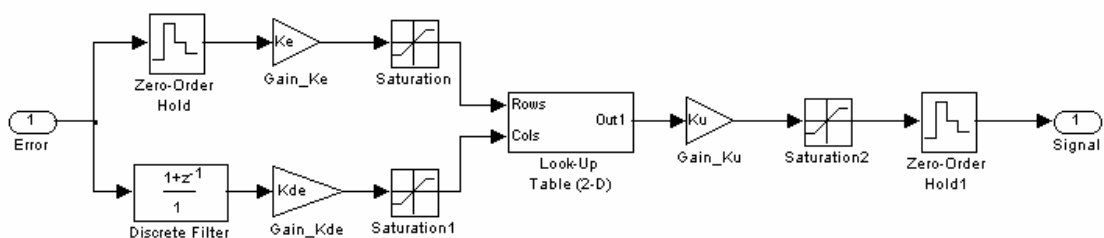


Figure 33: Simulink block diagram of the Fuzzy Logic Controller

Above block diagram contains two-dimensional *Look-Up Table* generated from the Fuzzy Logic Controller in Matlab[®]. It was necessary in order to apply FLC in real-time control with dSPACE[®] computer card. The table was created based on the input signals (position error and derivative of position error) with the intervals of 0.05. Input values between the 0.05 intervals are linearly interpolated in the look-up table block. Optimization of the controller can be done by changing the parameters of the gain blocks. In this experiment the best performance was received for the following values of the gains: $K_e = 65$ (error gain), $dK_e = 0.2$ (derivative of the error gain) and $K_u = 10$ (output gain).

Other blocks used in the above diagram are: the “Zero-Order Hold” block discretizing the continuous input signal by sampling the error and holding each value until the next sampling time, the “Discrete Filter” block that provides the derivative of the error between sampling times and three “Saturation” block – all with saturation limits set to 1 and -1. Input signal, the error, is the difference between the reference signal and the actual position of the piston.

Chapter 5 Experimental results

This chapter presents the experimental and simulation results of implementation a position-based impedance controller in controlling of hydraulic press. No problems were observed during the compilation and loading process between the Simulink[®] model used for *Real Time Workshop* (RTW) and dSPACE[®] computer card. The experimental data recorded by *ControlDesk* software was captured with the sample rate of 1 *ms* and saved as structured array. This format of data enabled later its analysis and formatting by using Matlab[®].

To enable the comparison of the results both experiment and simulation were conducted with the use of exactly the same parameters for the position controllers as well as identical impedance, which was implemented as a second order transfer function (equation 16)

$$M(s) = \frac{1}{Ms^2 + Bs + K} \quad (16)$$

where M is the desired mass, B is the desired dumping and K represents the desired stiffness.

Before the experiment with impedance control was conducted, both position controllers (PID and Fuzzy Logic Controller) were parameterized to achieve good precision trajectory control. Results of this parameterization for three different input signals (step, ramp and sinusoidal functions) are presented in section 5.1. The next section 5.2 contains result of the experiment and simulation with the position controllers parameterized before and impedance implemented to the force-feedback loop.

5.1. Position Control

Input signal – step function

Values of the parameters:

PID controller: $P = 0.3$, $I = 0.005$, $D = 0.0001$

Fuzzy Logic Controller: $K_e = 65$, $dK_e = 0.2$, and $K_u = 5$

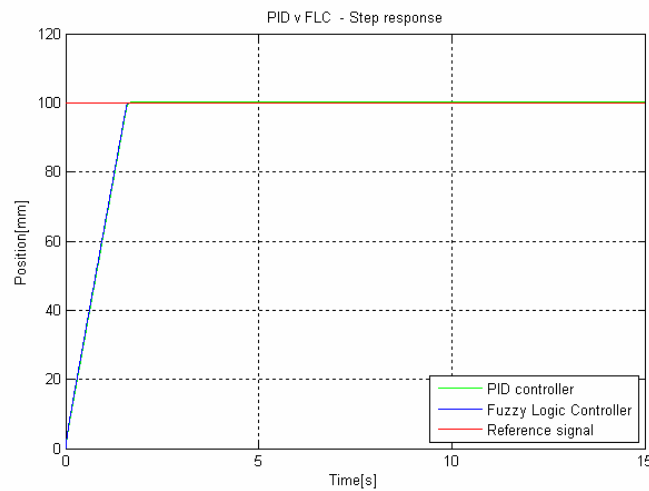


Figure 34: Position control - step input signal

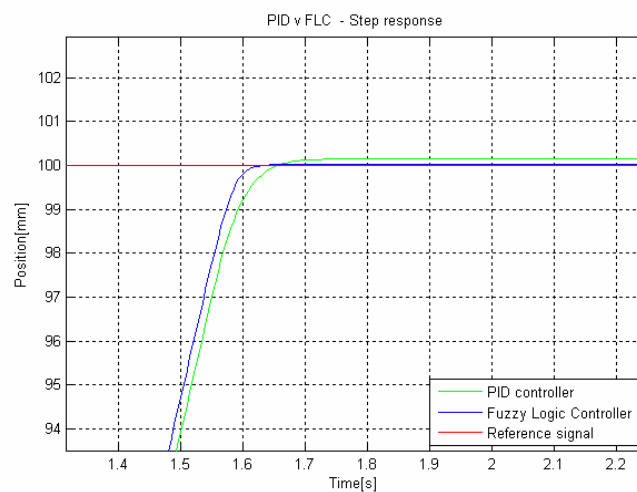


Figure 35: Position control - step input signal (zoom)

Above graphs present the response of the system on the step input signal. As can be seen FLC controller presents better performance than PID controller. System controlled by Fuzzy Logic Controller faster achieves desired position; moreover the steady state error is smaller than when PID controller was applied.

Input signal – ramp function

Values of the parameters:

PID controller: $P = 0.3$, $I = 0.005$, $D = 0.0001$

Fuzzy Logic Controller: $K_e = 65$, $dK_e = 0.2$, and $K_u = 5$

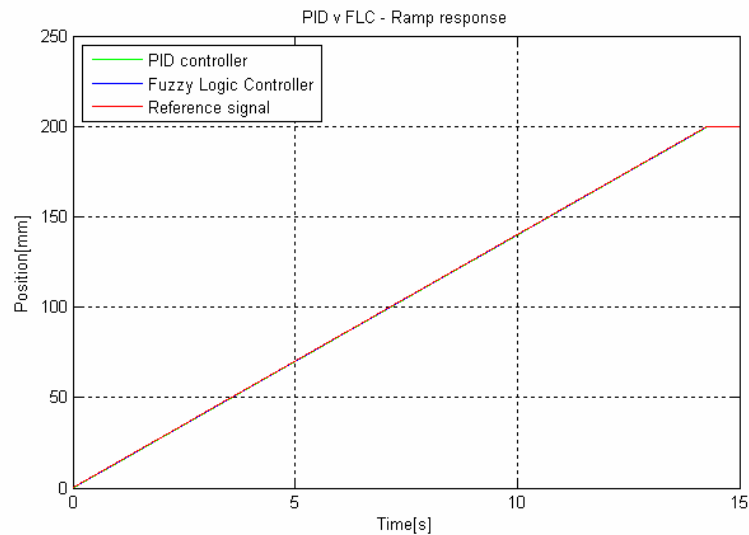


Figure 36: Position control - ramp input signal

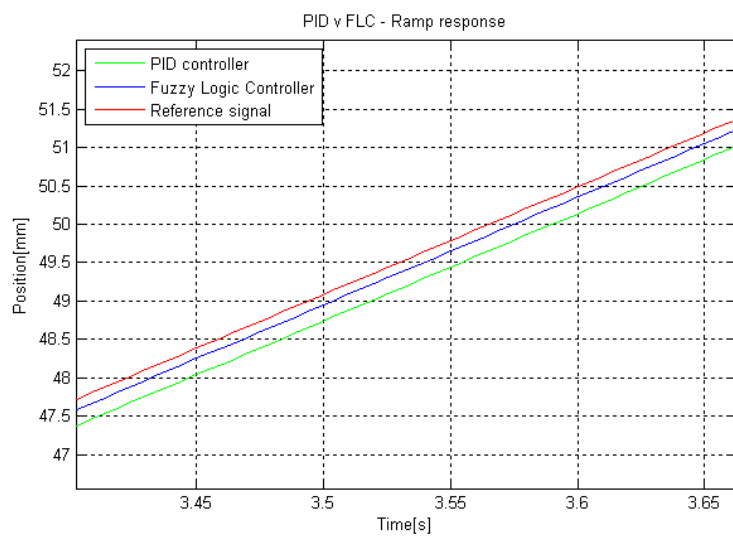


Figure 37: Position control - ramp input signal (zoom)

Above graphs present the response of the system on the ramp function input signal. In this case PID controller gave worst results than FLC controller. For Fuzzy Logic Controller the position error was less than 0.5, when the PID controller was used the position error was almost twice bigger.

Input signal – sinusoidal function

Values of the parameters:

PID controller: $P = 0.3$, $I = 0.005$, $D = 0.0001$

Fuzzy Logic Controller: $K_e = 65$, $dK_e = 0.2$, and $K_u = 5$

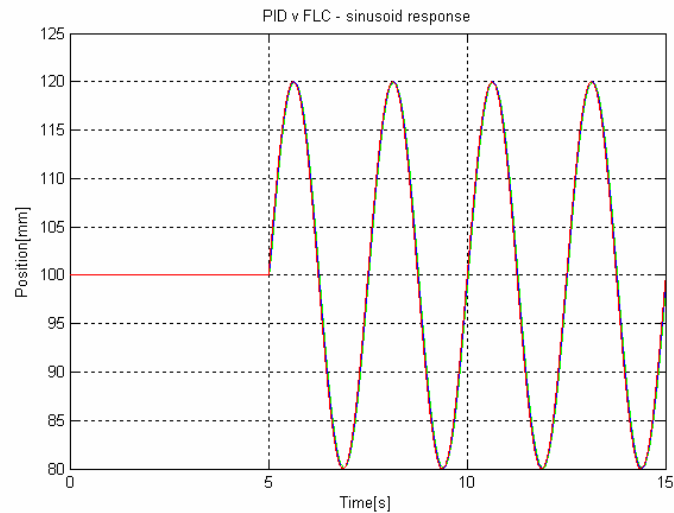


Figure 38: Position control - sinusoid input signal

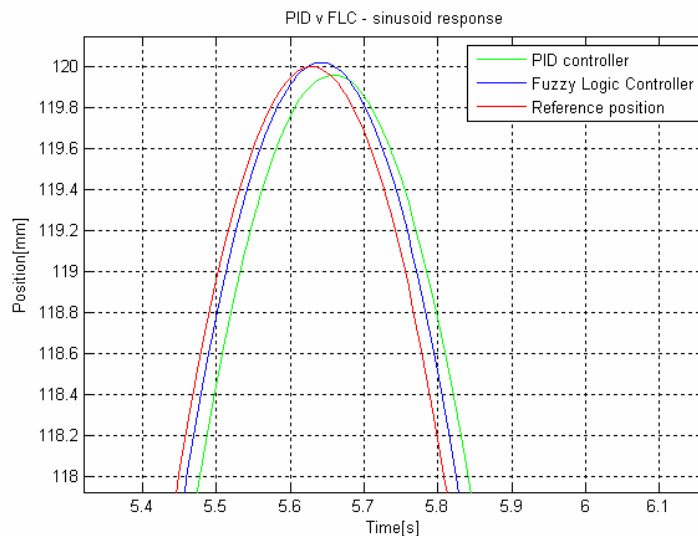


Figure 39: Position control - sinusoid input signal (zoom)

Above graphs present the response of the system on the sinusoidal function input signal. The performance of both position controllers was satisfactory. The position control done by FLC controller was more precise than performed by PID controller. In the situation when the reference signal was changing constantly, Fuzzy Logic Controller was reacting faster and gave smaller error.

5.2. Impedance Control

After the parameterization of the position controllers, the position-based impedance controller was implemented to the system by introducing a second order transfer function (equation 16) to the force-feedback loop. Experiments were conducted for two impedances with different values of the parameters (equation 17 and 18):

$$M_1(s) = \frac{1}{s^2 + 1000s + 1000000} \quad (17)$$

$$M_2(s) = \frac{1}{s^2 + 100s + 1500000} \quad (18)$$

Results were plotted and are displayed in this section. Graphs are organized in the following way: First two graphs (Figure 40 and 41) show the comparison of the reference trajectory of the punch and the trajectories registered during the experiment and simulation with ramp input signal where PID controller and implemented impedance $M_1(s)$ were used. Figures 42 and 43 present the result of the experiment in which the punch was in a constant position and a random environmental force was applied. The impedance introduced to force-feedback loop was $M_1(s)$ and $M_2(s)$ respectively. Next four graphs (Figure 44, 45, 46 and 47) present the results of the same experiments however the PID controller was replaced by a Fuzzy Logic Controller. Comparison of the experimental results and computer simulation results for both position controllers with a ramp function input signal and impedance $M_1(s)$ are presented in Figure 48 and 49. Figures 50, 51 and 52, 53 show the experimental results for the impedance $M_2(s)$ when ramp function and sinusoidal function were applied as reference signals. Results for the sinusoidal function and impedance $M_1(s)$ are shown in Figure 54. Last graph (Figure 55) shows the comparison of the hydraulic pressure in chamber A and B during the experiment as well as the simulation when a ramp function was applied to the system.

5.2.1. Position trajectory - PID controller

Input signal – ramp function

$$\text{Impedance: } M_1(s) = \frac{1}{s^2 + 1000s + 1000000}$$

PID controller: P = 0.1, I = 0.0002, D = 0.0001

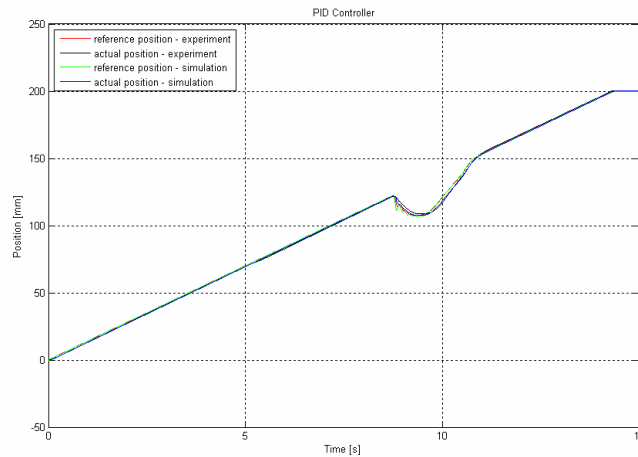


Figure 40: Position trajectory – ramp input signal – PID controller

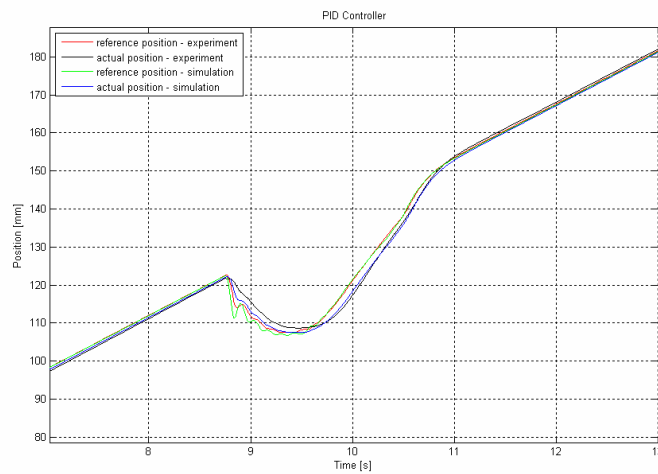


Figure 41: Position trajectory – ramp input signal – PID controller (zoom)

The response of the system to the ramp function input signal modified by the detected environmental force is presented above. That position control during the experiment gave good results. The similarity between the experimental results and simulation results can be noticed.

Constant position of the punch: 170mm

Random environmental force

$$\text{Impedance: } M_1(s) = \frac{1}{s^2 + 1000s + 1000000}$$

PID controller: P = 0.1, I = 0.0002, D = 0.0001

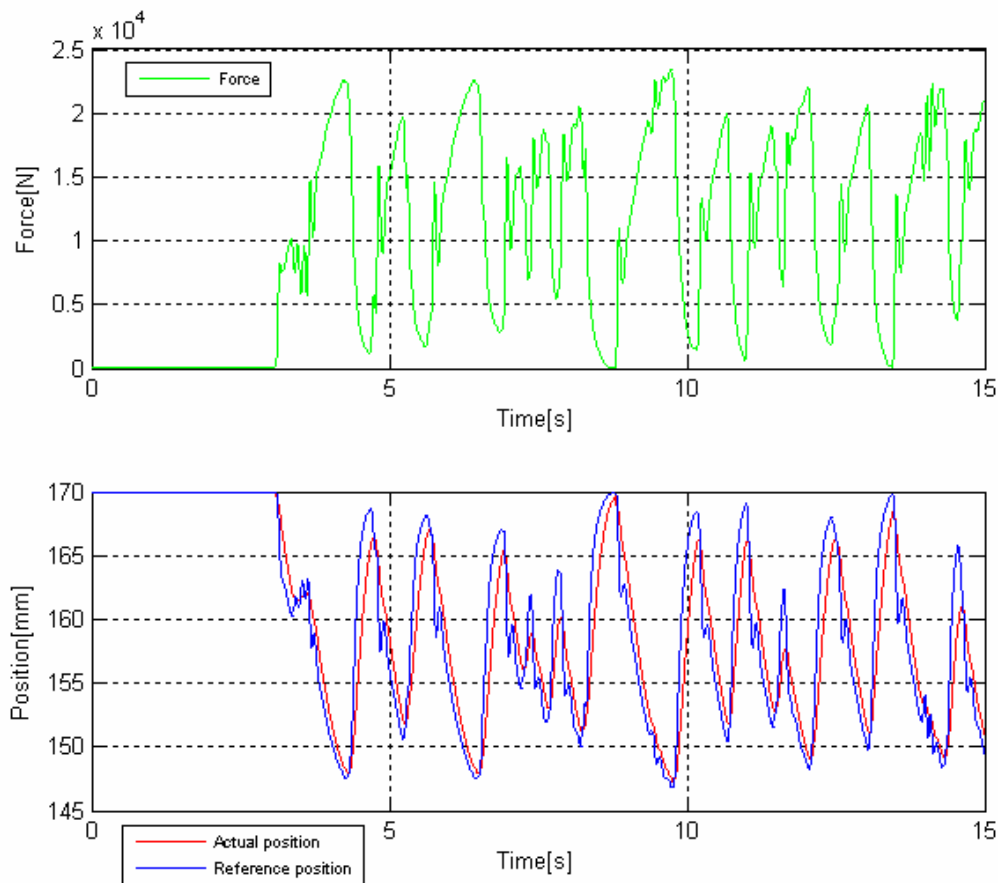


Figure 42: Constant position of the punch and random env. force – PID controller

In the experiment, which results are presented above, the constant value of the reference signal was applied to the system. Lower graph shows good performance of the PID controller on fast changes of the environmental force (presented in the upper graph). The actual trajectory of the punch, controlled by the PID position controller, was smoother than the reference signal.

Constant position of the punch: 170mm

Random environmental force

$$\text{Impedance: } M_2(s) = \frac{1}{s^2 + 100s + 1500000}$$

PID controller: P = 0.1, I = 0.0002, D = 0.0001

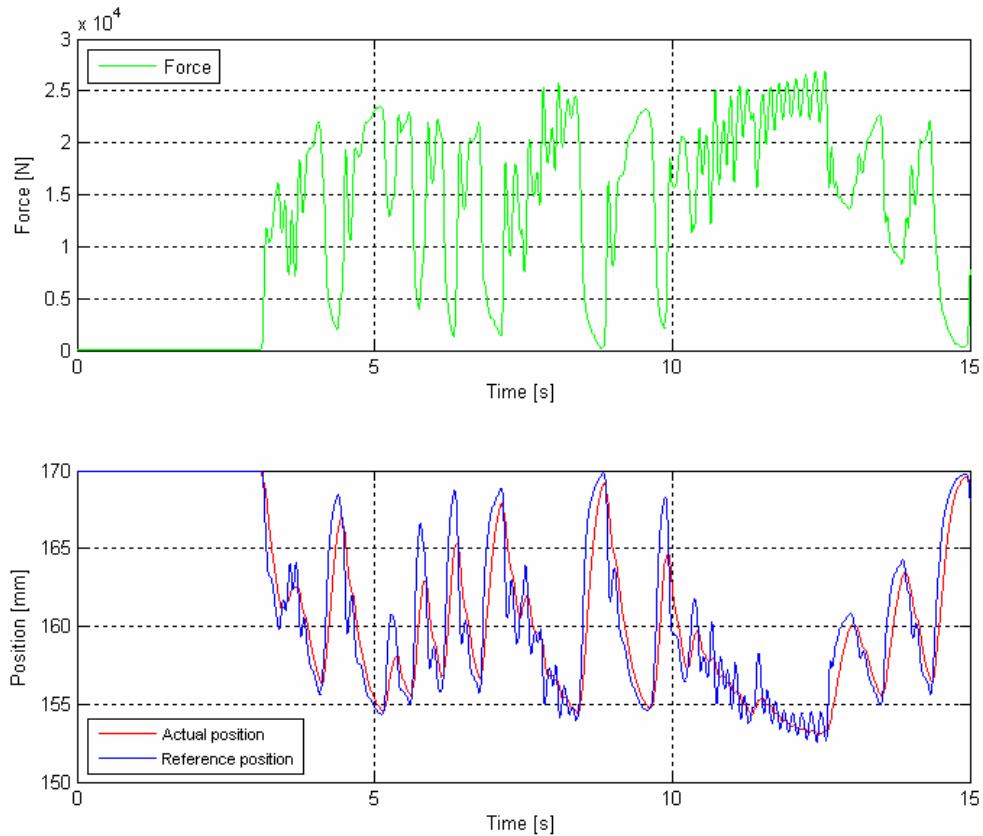


Figure 43: Constant position of the punch and random env. force – PID controller

These two graphs present the result of the same experiment; however for the different values of the impedance parameters. In both cases the reference signal was correctly modified according to the random changes of the environmental force.

5.2.2. Position trajectory – Fuzzy Logic Controller

Input signal – ramp function

$$\text{Impedance: } M_1(s) = \frac{1}{s^2 + 1000s + 1000000}$$

Fuzzy Logic Controller: $K_e = 10$, $dK_e = 0.2$, and $K_u = 5$

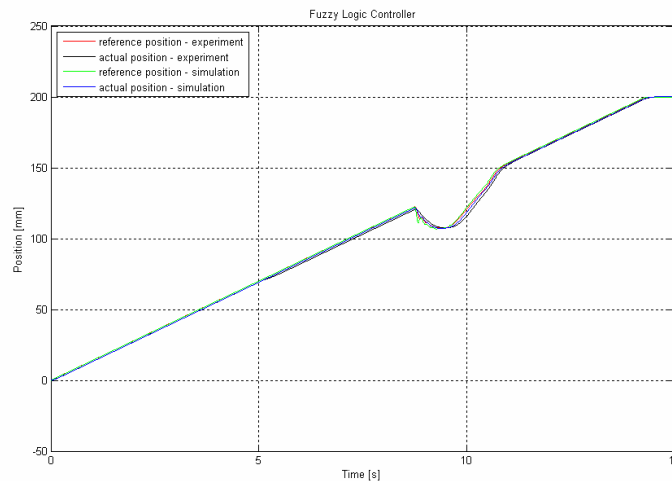


Figure 44: trajectory – ramp input signal – FLC controller

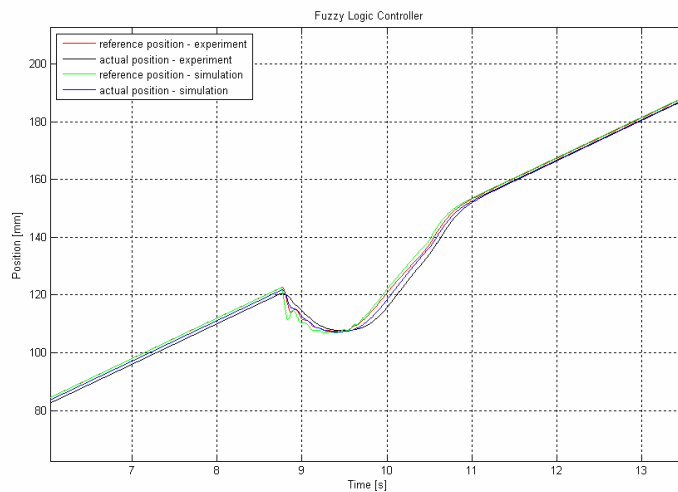


Figure 45: trajectory – ramp input signal – FLC controller (zoom)

Application of the Fuzzy Logic Controller gave good results, what can be seen in the above graphs. Also in this case computer simulation results were very similar to the results received during the experiment on real system although the position error in the experiment was slightly bigger than the error measured in simulation.

Constant position of the punch: 170mm

Random environmental force

$$\text{Impedance: } M_1(s) = \frac{1}{s^2 + 1000s + 1000000}$$

Fuzzy Logic Controller: $K_e = 10$, $dK_e = 0.2$, and $K_u = 5$

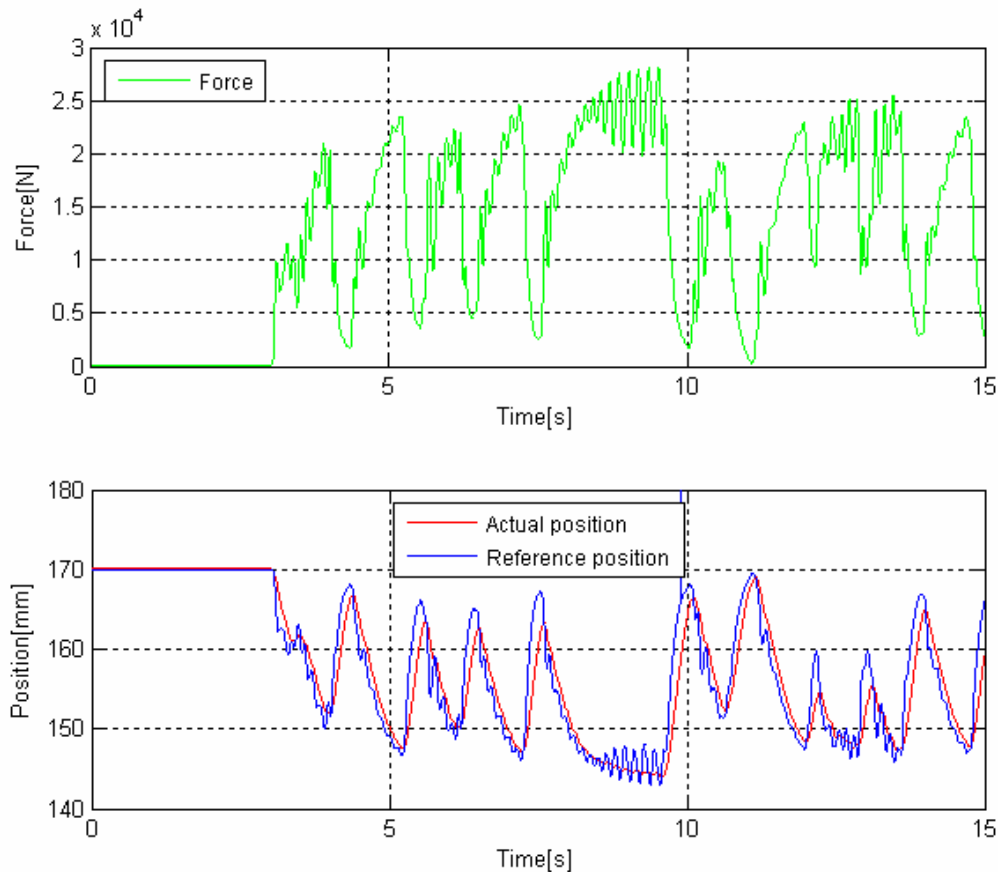


Figure 46: Constant position of the punch and random env. force – FLC controller

Above graphs as well two graphs presented on the next page present the response of the system to the constant value of the reference signal and random and fast changing environmental force. The position of the punch is modified after 3 seconds when the environmental force is detected. The changes of the actual position are softer than the changes of the reference signal.

Constant position of the punch: 170mm

Random environmental force

$$\text{Impedance: } M_2(s) = \frac{1}{s^2 + 100s + 1500000}$$

Fuzzy Logic Controller: $K_e = 10$, $dK_e = 0.2$, and $K_u = 5$

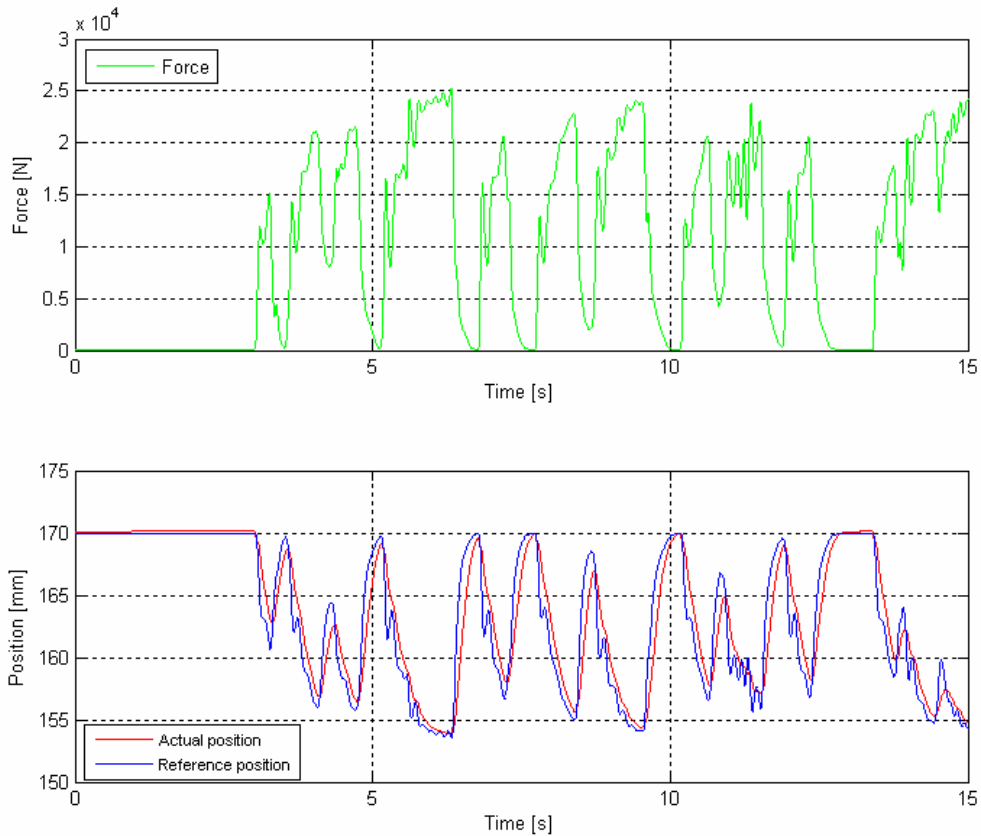


Figure 47: Constant position of the punch and random env. force – FLC controller

These two graphs show the results for different impedance implemented to the system. In both cases the results are satisfactory; however in this case the position error is smaller. Fuzzy Logic Controller smoother the actual trajectory of the punch especially when the reference signal changes very fast and the amplitude of changes is small.

5.2.3. Position trajectory – PID v FLC

Input signal – ramp function

$$\text{Impedance: } M_1(s) = \frac{1}{s^2 + 1000s + 1000000}$$

PID controller: P = 0.1, I = 0.0002, D = 0.0001

Fuzzy Logic Controller: Ke = 10, dKe = 0.2, and Ku = 5

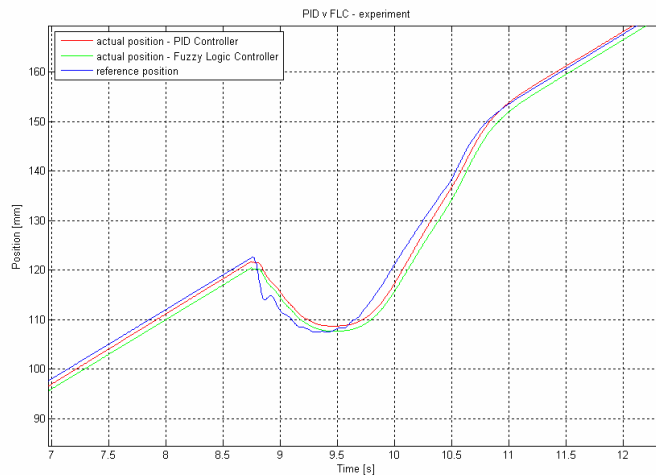


Figure 48: Position trajectory – ramp input signal – PID v FLC - experiment

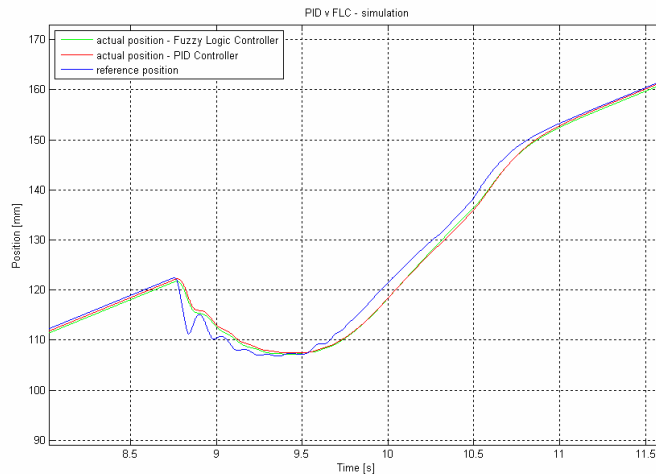


Figure 49: Position trajectory – ramp input signal – PID v FLC - simulation

As can be seen above, PID controller as well as Fuzzy Logic Controller gave acceptable results. Higher similarity in performance was noted during the simulation where the position error was also smaller for both controllers.

Input signal – ramp function

$$\text{Impedance: } M_2(s) = \frac{1}{s^2 + 100s + 1500000}$$

PID controller: P = 0.1, I = 0.0002, D = 0.0001

Fuzzy Logic Controller: Ke = 10, dKe = 0.2, and Ku = 5

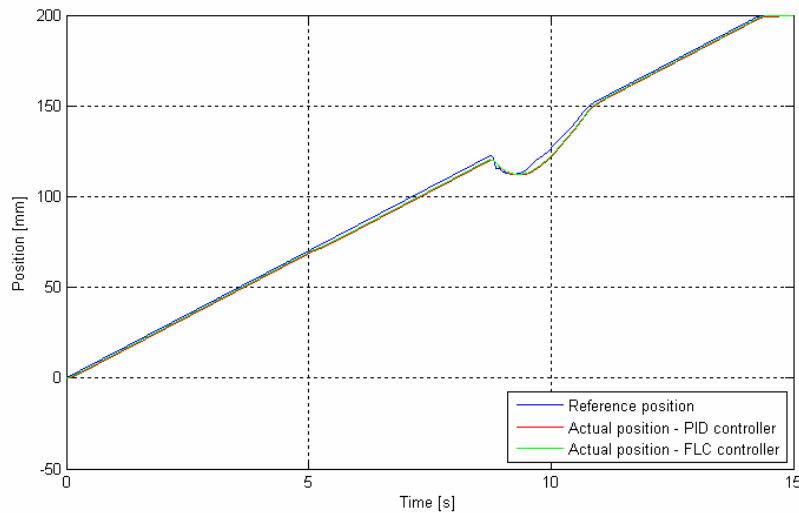


Figure 50: Position trajectory – ramp input signal – PID v FLC - experiment

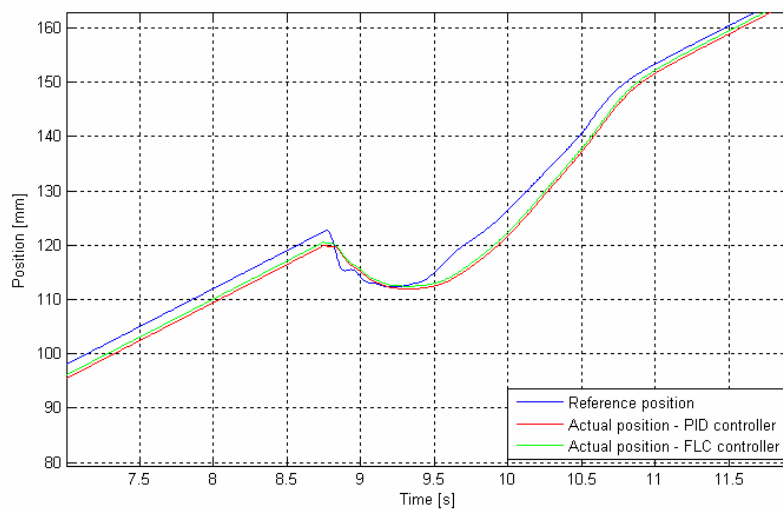


Figure 51: Position trajectory – ramp input signal – PID v FLC – exp. (zoom)

Comparison of the results, for both position controllers and second impedance $M_2(s)$ on the ramp function input signal, shows that the performances of both controllers is very similar; however the position error is bigger than in case of the first impedance $M_1(s)$.

Input signal – sinusoidal function

$$\text{Impedance: } M_2(s) = \frac{1}{s^2 + 100s + 1500000}$$

PID controller: P = 0.1, I = 0.0002, D = 0.0001

Fuzzy Logic Controller: Ke = 10, dKe = 0.2, and Ku = 5

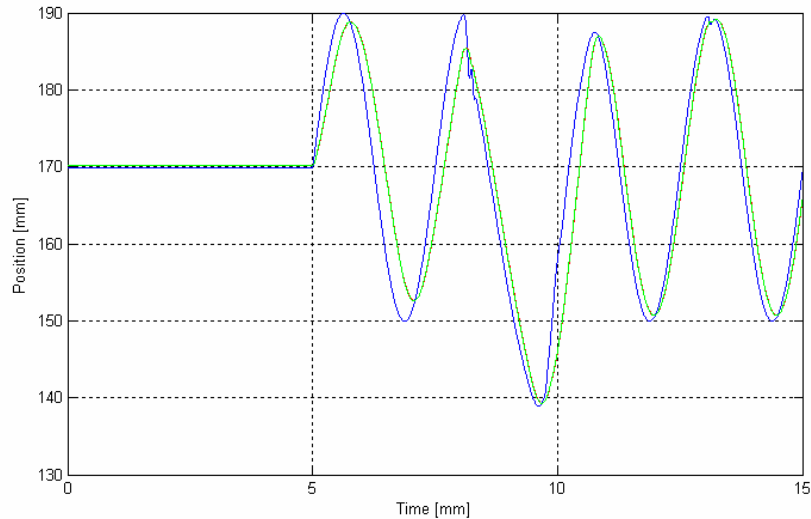


Figure 52: Position trajectory – sinusoid input signal – PID v FLC – experiment

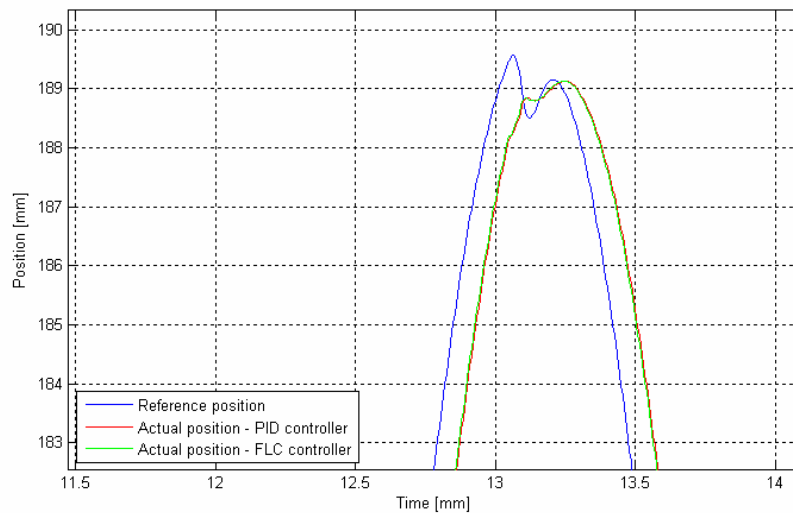


Figure 53: Position trajectory – sinusoid input signal – PID v FLC – exp. (zoom)

Sinusoidal signal with constant amplitude applied to the input of the system was modified by the environmental force. The position error at the beginning quite big after few seconds became smaller and the precision of position control performed by PID and FLC controller was acceptable.

Input signal – sinusoidal function

$$\text{Impedance: } M_1(s) = \frac{1}{s^2 + 1000s + 1000000}$$

PID controller: P = 0.1, I = 0.0002, D = 0.0001

Fuzzy Logic Controller: Ke = 10, dKe = 0.2, and Ku = 5

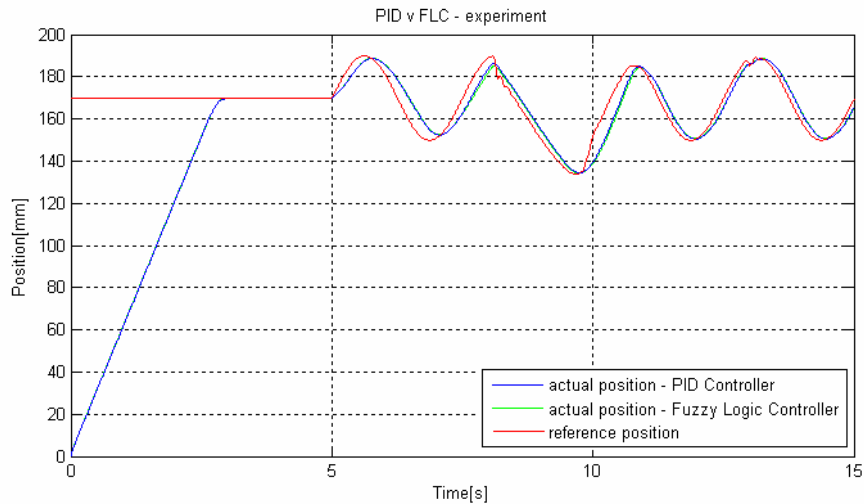


Figure 54: Position trajectory – sinusoid input signal – PID v FLC - experiment

5.2.4. Hydraulic pressure in chamber A and B

Input signal – ramp function

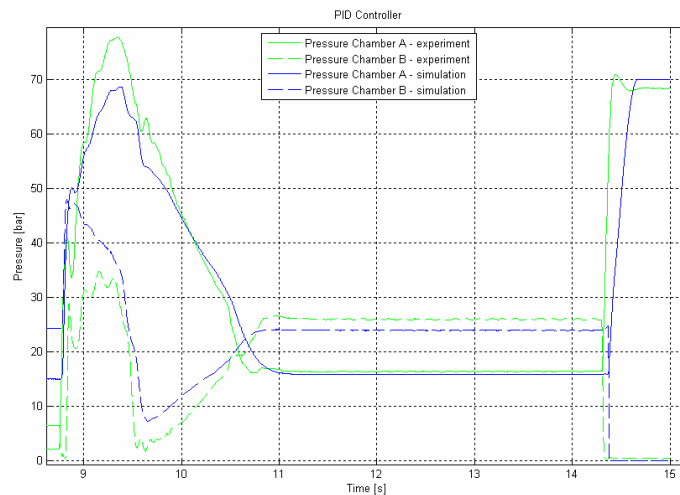


Figure 55: Hydraulic pressure in chamber A and B - exp. v sim. - PID controller

As can be seen above the changes of the hydraulic pressure in chamber A and B during the experiment and received in computer simulation are significantly similar.

5.3. Results Evaluation

The purpose of implementation position-based impedance controller is to adjust position of the hydraulic actuator according to the dynamic relation between the system endpoint position and the environmental contact force. This aim was achieved by implementing a second order transfer function to the force-feedback loop.

First task after the creating of the system was to parameterize the position controllers used in internal position control loop. Parameters and general performance of the controllers were tested by applying three different input signals to the system: step, ramp and sinusoid. As can be seen in Figures 34, 36 and 38 both PID and Fuzzy Logic Controller had good precision which means that parameters were chosen correctly. Fuzzy Logic Controller gave better results during the dynamic changes of the reference signal (see Figure 39) as well as smaller steady state error (see Figure 35).

When the position controllers were correctly parameterized the impedance loop was implemented. Three reference signals were applied to the system: linear function (a ramp), sinusoidal function and a constant value. As can be seen in the graphs in paragraph 5.2 the desired trajectory was modified when the impedance was implemented in the system. In the experiments when the ramp and sinusoid signals were applied the difference can be seen from around 8.5 second. It is the moment in which the load cell installed on the punch starts to detect environmental force (simulated by the press blank holder). As long as load cell has no contact with the blank holder the environmental force is equal to zero and the impedance has no influence on the setpoint. In Figure 42 and 47 actual and reference trajectory was compared with the randomly generated environmental force. In both cases the reference trajectory is modified according to the fast changes of measured force. Actual position of the punch is controlled correctly by both PID and Fuzzy Logic controllers, even when environmental force was changing very fast.

Experiments were conducted for two different sets of impedance parameters. First impedance had higher desired dumping factor and lower desired stiffness, in second case the desired dumping factor was ten times smaller however desired stiffness was higher. Implementation of the second impedance gave more smooth reference trajectory, however the position control gave worst results.

The position control performed by PID as well as Fuzzy Logic Controller gave good results. The Figure 48 shows that in both cases actual trajectory of the punch was very similar to the desired trajectory. It can be noticed that the actual paths of the punch were smoother from the reference for both controllers.

Computer simulation, conducted in Matlab/Simulink environment with the use of semi-empirical non-linear model of hydraulic system, after the model parameterization, gave also expected results. Figures 41 and 45 show a satisfactory similarity between the results of impedance control during the simulation and experiment. Position trajectory controlled by PID controller during the experiment is almost exactly the same as position of the punch generated during the computer simulation. The same situation could be observed when FLC controller was applied.

Pressure sensors, installed in the hydraulic cylinder, gave the opportunity to record the changes of hydraulic pressure in chamber A and B. The results of the measurements were presented in Figure 55. Also this graph shows a significant similarity between both experimental results and computer simulation results.

Chapter 6 Conclusion

The main purpose of this thesis was to develop and implement an impedance control for a hydraulic servomechanism. Based on the graphical results and empirical observation the general results of the experiment as well as computer simulation can be evaluated as good. System correctly adjusted the reference position of the punch according to the applied environmental force and implemented impedance. Both controllers (PID and Fuzzy Logic), used in position control, gave stable and satisfactory performance. The main objective of the thesis can be considered as fulfilled.

The comparison of the results received in experiment as well as computer simulation, presents a good similarity between the performance of real system and non-linear model used in simulation. Above observation shows that semi-empirical non-linear model of the hydraulic system, after a correct parameterization, can successfully replace a real system in computer simulation. This solution enables a computer offline parameterization of the controllers, without exposing real equipment to the risk, in case of undesirable behavior of the system.

Although Fuzzy Logic Controller is non-linear, the development and implementation, with the use of standard fuzzy logic controller setup provided by Matlab, did not cause many problems. In case of controlling of non-linear, uncertain dynamic systems, like hydraulic systems, FLC can be successfully applied, giving good performance characteristics. Second controller used in the experiment was a PID controller. This very popular and well-studied linear controller, despite of its weakness in many high-performance applications, is widely compared against with other controllers. In this experiment PID controller met its requirements, positioning the system with acceptable precision.

Research literature says that performance of position-based impedance controller depends significantly on the precision of internal position controller. During the experiment when the position controllers parameterized before were implemented to the impedance controller, the undesirable oscillations of the system occurred. To

achieve good behavior of the system parameters of the position controllers both PID and Fuzzy Logic controllers had to be changed. Also when the values of the impedance parameters were changed to smaller the oscillations increased. The explanation of this unexpected behavior of the system can be the way how the environmental force is measured. Load cell used in the experiment to measure the environmental force is an analog device sensitive to external noise that could be introduced later to the system. Other explanation of this situation can be the type of the impedance that was used. The impedance implemented to the force-feedback loop is a linear second order transfer function. Alternative solution would be applying the generalized impedance [Bilodeau98] that could remove the problems mentioned above. This idea was not verified in this work.

The hydraulic press where the experiment was conducted on is well equipped with all necessary data acquisition instruments and sensors, which allowed performing the task and collects all data, needed for further analysis. During the experiment, due to the external noises, hydraulic press was going into oscillations. This problem, which did not occur during the computer simulation, was solved by applying filters in the system. The filters implemented to each signal from the sensors as well as in force-feedback loop, removed noise and enabled to perform the experiment and acquired precise data.

It has to be point out that Real Time Interface - *ControlDesk*[®] software provided by dSPACE[®] proved its usefulness and in easy and fast way enabled to develop an interface for the monitoring and acquisition of data during the experiment. Possibility of changing control parameters and press operations in real time, without constant compilation of ANSI C code, simplified the procedure of parameterization and optimization of the system and position controllers.

The position-based impedance controller developed and implemented in this work is only one type of impedance control. As an extension to this work and using the models developed by the author, the force-based impedance controller could be implemented. Hydraulic press contains all necessary equipment and sensors (e.g. load cell installed on the punch that can directly measure the force) to conduct this experiment and record the results that could be compared with the results presented in

this work. Also additional tests could be made with the use of different position controllers (e.g. model-based predictive control) and other reference signals. This work could be extended as well by implementing generalized impedance in the force-feedback loop that could eliminate undesirable oscillations observed during the experiment.

In future projects, the same procedure that was described in this work can be applied to control other hydraulic servomechanisms located at the University of Aveiro. The non-linear model has to be parameterized individually in each case however the methodology of controller implementation is the same.

References

[Alleyne95] - Alleyne, A., and J. K. Hedrick, *Nonlinear Adaptive Control of Active Suspensions*, IEEE Transactions on Control Systems Technology, Vol. 3, No. 1, pp. 94-101, March 1995.

[Becker95] - Becker, U. *The behaviour of a position controlled actuator with switching valves*. In Proceedings of Fourth Scandinavian International Conference on Fluid Power, Tampere, Finland, pp. 160-167, 26-29 September 1995.

[Bilodeau98] – Bilodeau, G., Papadopoulos, E., *A Model-Based Impedance Control Scheme for High-Performance Hydraulic Joints*, Proceedings of the 1998 IEEE/RSJ Intl. Conference on Intelligent Robots and Systems, Victoria, B.C., Canada, pp. 1308-1313, October 1998

[Cho04] – Cho, H. and Yi, S-J., *Vehicle trajectory control using the fuzzy logic controller*, In Proc. Instn Mech. Engrs Vol. 218 Part D: J. Automobile Engineering, pp. 21-32, 2004

[Clegg00] - Clegg, A., *Self-tuning Position and Force Control of a Hydraulic Manipulator*, Doctoral Thesis, Department of Computing and Electrical Engineering, Heriot-Watt University, United Kingdom, 2000.

[Cubero00] - Cubero, S. N., *A 6-Legged Hybrid Walking And Wheeled Vehicle*, 7th International Conference on Mechatronics and Machine Vision in Practice, Hervey Bay, QLD, Australia, September pp. 293-302, 19 - 21, 2000.

[Daley87] - Daley, S., *Application of a fast self-tuning control algorithm to a hydraulic test rig*, Proc. Instn Mech. Engrs, Part C, 201(C4), pp. 285-295, 1987.

[Dorf95] - Dorf, R. C. and Bishop, R. H., *Modern Control Systems*, 7th edition, , pp. 648 et seq., Addison-Wesley, London, 1995.

[Durfee09] - Durfee W., and Z. Sun, *Fluid Power Systems Dynamics*, A National Science Foundation, pp. 1-8, 2009.

[Edge87] - Edge, K. A. and Figueredo, K.R.A., *An adaptively controlled electrohydraulic servo-mechanism. Part 1: Adaptive controller design, Part 2: implementation*, Proc. Instn Mech. Engrs, Part B, 201(B3), pp. 175-189, 1987.

[Edge95] - Edge, K. A. and de Almeida, F. G. *Decentralised adaptive control of a directly driven hydraulic manipulator. Part 1: theory, Part 2: experiment*, Proc. Instn Mech. Engrs, Part I, 209(I3), pp. 191-205, 1995.

[Edge97] - Edge, K.A., *The Control of Fluid Power Systems – Responding to the Challenges*, Proc. Instn. Mech. Engrs., Vol 211 (91-110), Part I: Journal of Systems and Control Engineering, 1997, (United Kingdom Automatic Control Council Lecture, 1996).

[Ferreira02] - Ferreira, J.A., Gomes de Almeida, F. and Quintas, M.R., *Semi-Empirical Model For A Hydraulic Servo-Solenoid Valve*, Proc. Instn Mech. Engrs, Part I, Journal of Systems and Control Engineering, Vol 216, pp. 237-248, 2002.

[Ferreira03] - Ferreira, J.A., *Modelação de Sistemas Hidráulicos para Simulação com Hardware-in-the-loop*, Doctoral Thesis, Departamento de Engenharia Mecânica, Universidade de Aveiro, Portugal, 2003.

[Ferreira04] - Ferreira, J.A., Gomes de Almeida, F. and Quintas, M.R., *Hybrid models for hardware-in-the-loop simulation of hydraulic systems. Part 1: theory*, Proc. Instn Mech. Engrs, Part I, Journal of Systems and Control Engineering, Vol. 218, pp. 465-474, 2004.

[Ferretti04] - Ferretti, G., Magnani, G., Rocco, P., *Impedance Control for Elastic Joints Industrial Manipulators*, IEEE Transactions on Robotics and Automation, Vol. 20, No. 3, June 2004.

[French04] - French, C. W., Shultz, A. E. Hajjar, J.F., *Multi-Axial subassemblage Testing (MAST) System: Description and Capabilities*, 13th World Conference on Earthquake Engineering, Vancouver, B.C., Canada, Paper No. 2146, August 1-6, 2004.

[Friedland86] - Friedland, B., *Control System Design- An Introduction to State Space Methods*, McGraw-Hill, London, 1986.

[Gardner95] - Gardner, J. F., et al., *Modelling and Tuning of Hydraulic Road Simulators for Heavy Vehicle Testing*, Fluid Power Systems and Technology, Vol. 2, pp. 99-105, Collected papers presented at the 1995 ASME International Mechanical Engineering Congress and Exposition, San Francisco, CA, November 1995.

[Habibi91] - Habibi, S. R. and Richards, R. J. *Computed-torque and variable-structure multi-variable control of a hydraulic industrial robot*, Proc. Instn Mech. Engrs, Part I, , 205(I2), pp. 123-140, 1991.

[Harris94] - C.J. Harris, *Advances in intelligence control*, Taylor & Francis, 1994.

[Hogan85] - Hogan N., *Impedance Control: An Approach to Manipulation*, Parts I-ID, ASME Journal of Dynamic Systems, Measurement, and Control, vol. 107, pp. 1-24, 1985.

[Klein95] - Klein, A. and Backe Â, W., *An intelligent optimisation of a state loop controller with fuzzy-set-logic. In Circuit, Component and System Design*, Proceedings of Fifth Bath International Fluid Power Workshop, (Eds C. R. Burrows and K. A. Edge), (Research Studies Press), pp. 381-399, 1995.

[Lennevi95] - Lennevi, J. and Palmberg, J.-O. *Application and implementation of LQ design method for the velocity control of hydrostatic transmissions*, Proc. Instn Mech. Engrs, Part I, 209(I4), pp. 255-268, 1995.

[Lin90] - Lin, S.J., and Akers A., *Optimal Control Theory Applied to Pressure-Controlled Axial Piston Pump Design*, ASME Journal of Dynamic Systems, Measurement and Control, Vol. 112, No. 3, pp. 475-481, 1990.

[Liu93] - Liu, P. and Dransfield, P. *Intelligent control of air servodrives using neural networks*, In Fluid Power, Proceedings of Second JHPS International Symposium on Fluid Power (Ed. T. Maeda), E. & N. Spon, London, pp. 743-748, 1993.

[Mamdani75] - Mamdani, E.H. and Assilian S., *An experiment in linguistic synthesis with a fuzzy logic controller*, International Journal of Man-Machine Studies, Vol. 7, No. 1, pp. 1-13, 1975.

[McAllister95] - McAllister, J., *The control of cruciform testing systems using opposed pairs of servo-hydraulic cylinders*, In Innovations of Fluid Power, Proceedings of Seventh Bath International Fluid Power Workshop (Eds C. R. Burrows and K. A. Edge), (Research Studies Press), pp. 311-320, 1995.

[Mayer92] - Mayer, E. A., *Analytical Evaluation of Servovalves for Flight Simulator Motion Bases*, The Journal of Fluid Control, Vol. 21, Issue 2-3, pp. 27-47, 1992.

[Newton95] - Newton, D. A., *Application of a neural network controller to control a rotary drive system with high power efficiency*. In Innovations in Fluid Power, Proceedings of Seventh Bath International Fluid Power Workshop (Eds C. R. Burrows and K. A. Edge), (Research Studies Press), pp. 41-54, 1995.

[Niemela95] - Niemela, E. and Virvalo, T., *Usage of fuzzy logic in hydraulic servo*, In Proceedings of Fourth Scandinavian International Conference on Fluid Power, Tampere, Finland, pp. 119-132, 26-29 September 1995.

[Paoluzzi95] - Paoluzzi, R., Zarotti, L. G. and Ferretti, G., *Multiple hybrid control of pump displacement*, In Fourth Scandinavian International Conference on Fluid Power, Tampere, Finland, pp. 605-617, 26-29 September 1995.

[Piche91] - Piche Â, R., Pohjolainen, S. and Virvalo, T., *Design of robust controllers for position servos using H-infinity theory*, Proc. Instn Mech. Engrs, Part I, 205(I4), pp. 299-306, 1991.

[Piche92] - Piche, R., Pohjolainen, S. and Virvalo, T., *Design of robust two-degree of freedom controllers for position control servos using H-infinity theory*, Proc. Instn Mech Engrs, Part I, Journal of Systems and Control Engineering, 206(I2), pp. 135-142, 1992.

[Plummer96] - Plummer, A. R., and Vaughan N. D., *Robust Adaptive Control for Hydraulic Systems*, ASME Journal of Dynamic Systems, Measurement, and Control, Vol. 118, No. 2, pp. 237-244, June 1996.

[Salcudean97] – Salcudean, S.E., Tafazoli, S., Lawrence, P. Chau, D.I., *Impedance Control of a Teleoperated Mini Excavator*, In Proc. of the 8th IEEE International Conference on Advanced Robotics (ICAR), 1997.

[Sanada93] - Sanada, K., Kitagawa, A. and Pingdong, W., *An application of a neural network to adaptive control of a servosystem*, In Fluid Power, Proceedings of Second JHPS International Symposium on Fluid Power (Ed. T. Maeda), (E. & N. Spon, London), pp. 303-308, 1993.

[Shih93] - Shih, M.-C. and Liaw, S.M., *Hydraulic servocylinder position control using a fuzzy logic controller*, In Fluid Power, Proceedings of Second JHPS International Symposium on Fluid Power (Ed. T. Maeda), (E. & N. Spon, London), pp. 279-284, 1993.

[Stroup81] - Stroup, N. G., and Krukow, E. J., *Hillside Axial-Flow Combine Hydraulic Systems*, Proceedings of the 37th National Conference on Fluid Power, Chicago, IL, 1981.

[Sugeon85] - Sugeno, M., *Industrial applications of fuzzy control*, Elsevier Science Pub. Co., 1985.

[Thollt95] - Thollot, J. *Adaptive control of a hydraulic cylinder- a system performance based approach*, In Innovations in Fluid Power, Proceedings of Seventh Bath International Fluid Power Workshop (Eds C. R. Burrows and K. A. Edge), (Research Studies Press), pp. 161-176, 1995.

[Wu95] - Wu, H.-W. and Lee, C.-B., *Self-tuning adaptive speed control of a pump/inverter controlled hydraulic motor system*, Proc. Instn Mech. Engrs, Part I, 209(I2), pp. 101-114, 1995.

[Vaughan86] - Vaughan, N. D. and Whiting, I. M., *Microprocessor control applied to a non-linear electrohydraulic position control system*, In Proceedings of Seventh International Fluid Power Symposium, pp. 219-229, 16-18 September 1986.

[Vaughan92] - Vaughan, N. D., and Gamble, J., *Sliding mode control of a proportional solenoid valve*, In Fluid Power Systems Modelling and Control, Proceedings of Fourth Bath International Fluid Power Workshop (Eds C. R. Burrows and K. A. Edge), (Research Studies Press), pp. 95-107, 1992.

[Virtanen93] - Virtanen, A., *The design of state controlled hydraulic position servo system*, In Proceedings of Third Scandinavian International Conference on Fluid Power, Linkoping, Sweden, pp. 193-206, 25-26 May 1993.

[Zadeh72] - Zadeh, L.A., *A rationale for fuzzy control*, J. Dynamic Syst. Meas. Control, vol.94, series G, pp.3-4, 1972.